High-Temperature Catalysts for the Production of α-Olefins Based on Iron(II) and Iron(III) Tridentate Bis(imino)pyridine Complexes with Double Pattern of Substitution: *ortho*-Methyl plus *meta*-Aryl†

Alex S. Ionkin,* William J. Marshall, Douglas J. Adelman, Barbara Bobik Fones, Brian M. Fish, and Matthew F. Schiffhauer

DuPont Central Research & Development, Experimental Station, Wilmington, Delaware 19880-0328

Received December 15, 2005

Four types of bis(imino)pyridine ligands and their corresponding Fe complexes with the same *meta*-aryl pattern were synthesized for high-temperature α-olefin production (**A**: **9** and **13**; **B**: **18**, **19**, **20** and **21**, **22**, **23**, **24**; **C**: **27** and **30**; and **D**: **33** and **34**). Pattern **A** (**9** and **13**) consists of four *meta*-aryl groups without *ortho*-methyls. The coordination of $FeCl_2$ with the ligand [3,5-bis(4-F-Ph)$_2$-Ph-N═C(Me)-Py-C(Me)═N-Ph-3,5-bis(4-F-Ph)$_2$] (**9**) of type **A** resulted in the isolation of ion-paired complexes $[L_2Fe]^{2+}FeCl_4^{2-}$ **13**. Coordination of ligands **18**, **19**, and **20** of pattern **B** with two *meta*-aryl groups on the same side with two *ortho*-methyls of the imino aryl group afforded the following 1:1 complexes: [{3-(4-F-Ph)-2-Me-Ph-N═C(Me)-Py-C(Me)═N-Ph-2-Me-3-(4-F-Ph)}$FeCl_2$] (**21**), [{3-(3,5-bis-$(CF_3)_2$-Ph)-2-Me-Ph-N═C(Me)-Py-C(Me)═N-Ph-2-Me-3-(3,5-bis-$(CF_3)_2$-Ph)}$FeCl_2$] (**22**), [{3-(3-Me-thiophene-2-yl)-2-Me-Ph-N═C(Me)-Py-C(Me)═N-Ph-2-Me-3-(3-Me-thiophene-2-yl)}$FeCl_2$] (**23**), and [{3-(3,5-bis-$(CF_3)_2$-Ph)-2-Me-Ph-N═C(Me)-Py-C(Me)═N-Ph-2-Me-3-(3,5-bis-$(CF_3)_2$-Ph)}$FeCl_3$] (**24**). Reduction of trivalent complex **24** in THF solution yields divalent complex **22**. Ligand **27** of pattern **C** contains two *meta*-aryl groups on the side opposite two *ortho*-methyls of the imino aryl group and coordinates with $FeCl_2$ to form complex [{5-(3,5-bis-$(CF_3)_2$-Ph)-2-Me-Ph-N═C(Me)-Py-C(Me)═N-Ph-2-Me-5-(3,5-bis-$(CF_3)_2$-Ph)}$FeCl_2$] (**30**). Complex **34** of unsymmetrical pattern **D** has two *meta*-aryls in one imino aryl group and two *ortho*-methyls in the second imino aryl group: [{2,6-dimethyl-4-(3,5-bis-$(CF_3)_2$-Ph)-2-Me-Ph-N═C(Me)-Py-C(Me)═N-Ph-2-Me-3,5-bis(3,5-bis-$(CF_3)_2$-Ph)}$FeCl_2$]. The introduction of aryl groups into the *meta* positions of all four types of bis(imino)pyridine ligands was accomplished by palladium-catalyzed Suzuki cross-coupling reaction between aryl boronic acid **5**, **16**, and **17** and the appropriate *meta*-bromo-substituted bis(imino)pyridine ligands **4**, **15**, **25**, and **32**. Di-*tert*-butyl(2,2-dimethylpropyl)phosphane (**7**) and benzyl-di-*tert*-butylphosphane (**28**) were used as ligands for the Suzuki coupling. According to X-ray analysis, there are shortenings and therefore strengthening of the axial Fe−N bond lengths (up to 0.02 Å) in complex **22** of type **B** versus the Fe(II) complex without *meta*-aryl groups [{*o*-Me-Ph-N═C(Me)-Py-C(Me)═N-Ph-*o*-Me}$FeCl_2$] (**1**). Complexes of patterns **B** and **D** (**21**, **22**, **23**, **24**, and **34**) afforded very active catalysts for the production of α-olefins with more ideal Schultz−Flory distributions of α-olefins and with higher *K* values than the parent methyl-substituted Fe(II) complex **1** without *meta*-aryl groups.

Introduction

Fe^{II} catalysts with tridentate bis(imino)pyridine ligands have been reported to afford α-olefin oligomers with perfect Schultz−Flory distributions, exceptional purities (97−99%), and high productivities.[1a−d] The results exceed values being reported for catalysts used in current commercial processes, including the original Ziegler's process and the Shell Higher Olefin Process (SHOP).[2] SHOP is a very efficient and flexible combination of multistep reactions: oligomerization, isomerization, and metathesis. The oligomerization component of SHOP is based on the neutral Ni^{II} complexes bearing bidentate P^O ligands. The SHOP process makes 96−98% α-olefins with 2−4% branched olefins.[2b,c] The absence of "chain walking" along the polymer chain with Fe^{II} catalysts is responsible for the high-quality of the α-olefin products. The corresponding Ni^{II} catalysts with α-diimine ligands, for example, offer only 94% selectivity for linear α-olefins due to the ability of nickel-based catalysts to chain walk and therefore to produce substantial amounts of branched α-olefins.[3] Currently, there is also a significant effort by Sasol to achieve selective production of 1-hexene and 1-octene based on Cr^{III} complexes.[4]

There is an advantage, with regard to toxicity, to using iron instead of nickel or chromium based catalytic systems.[5] The high catalyst activity of Fe^{II} Versipol catalysts also allows once-

† Dedicated to Dr. Joel D. Citron, a proponent of iron tridentate chemistry, on the occasion of his 65th birthday. This is DuPont contribution no. 8667.

* To whom correspondence should be addressed. E-mail: alex.s.ionkin@usa.dupont.com.

(1) For initial patents and publications see: (a) Bennett, A. M. A. (DuPont) PCT Int. Appl. WO9827124 A1, 1998, 68 pp. (b) Brookhart, M. S.; Small, B. L. PCT Int. Appl. WO 9902472 A1 1999, 54 pp. (c) Small, B. L.; Brookhart, M. *J. Am. Chem. Soc.* **1998**, *120*, 7143. (d) Britovsek, G. J. P.; Gibson, V. C.; Kimberley, B. S.; Maddox, P. J.; McTavish, S. J.; Solan, G. A.; White, A. J. P.; Williams, D. J. *Chem. Commun*. **1998**, 849. For recent reviews see: (e) Ittel, S. D.; Johnson, L. K.; Brookhart, M. *Chem. Rev.* **2000**, *100*, 1169. (f) Britovsek, G. J. P.; Gibson, V. C.; Wass, D. F. *Angew. Chem., Int. Ed.* **1999**, *38*, 428. (g) Mecking, S. *Coord. Chem. Rev.* **2000**, *203*, 325. (h) Gibson, V. C.; Spitzmesser, S. K. *Chem. Rev*. **2003**, *103*, 283.

(2) (a) Vogt, D. In *Applied Homogeneous Catalysis with Organometallic Compounds*; Cornils, B., Herrmann, W. Eds.; VCH Publishers: Weinheim, 1996; Vol. 1, p 245. (b) Lutz, E. F. *J. Chem. Educ.* **1986**, *63*, 202. (c) Vogt, D. In *Aqueuos-Phase Organometallic Catalysis*; Cornils, B., Herrmann, W. A., Eds.; VCH Publishers: Weinheim, 1998; p 541.

(3) Killian, C. M.; Johnson, L. K.; Brookhart, M. *Organometallics* **1997**, *16*, 2005.

10.1021/om051069o CCC: $33.50
Publication on Web 05/11/2006

Scheme 1

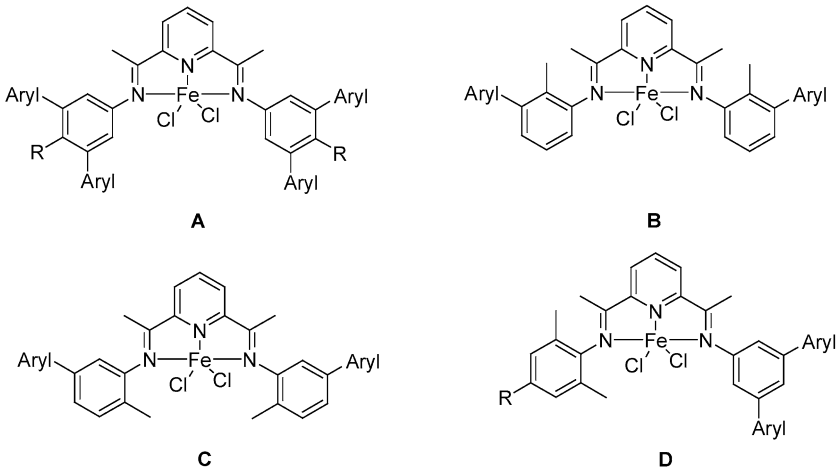

through oligomerization, eliminating the need for catalyst recycle or removal.[1e]

An early, leading candidate identified was Fe^{II} complex **1**, with a tridentate bis(imino)pyridine ligand bearing only one methyl group in the *ortho* positions of the imino aryl groups.[1c,e]

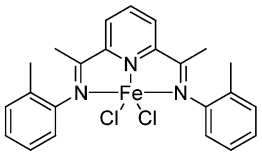

1

Careful analysis of the performance of complex **1** as a precatalyst over the commercially desirable temperature range of 100−120 °C revealed some significant shortcomings. For example, while complex **1** is extremely productive, its lifetime at 120 °C is only 3 min. Its high productivity is desirable, but, for injection into a plug-flow reactor, a less active catalyst with a longer lifetime would be preferred. This would make generation of an undesirable "hot-spot" at the injection point less likely and would reduce the number of injection points needed.

Another concern was the product distribution obtained using the catalyst derived from complex **1**. The oligomer distribution deviated from Schultz−Flory at the low and high MW ends. For a general commercial application in which C_6 to C_{16} α-olefins are targeted, it is desirable to minimize the production of butene, in particular, and of oligomers of $>C_{16}$. They have limited commercial value and represent an ethylene yield loss. These species were instead enhanced by the use of complex **1**. The goal of this work was to synthesize and test catalysts with several alternative substitution patterns on the imino aryl groups to see if a more thermally stable candidate with a near ideal Schultz−Flory distribution of oligomers could be discovered.

Four new generic patterns of the substitutions in the ligands of Fe^{II} tridentate complexes (Scheme 1) were reasoned to make complexes more thermally stable by increasing remotely the steric protection around the metal with a high degree of precision. All of them have a similar feature: a *meta*-aryl group. Additional placement of a sterically bulky group in vacant *ortho* positions, close to the catalytically active center, changes the process completely from ethylene oligomerization to polymerization.[6] Pattern **A** consists of four *meta*-aryl groups without *ortho*-methyls. Pattern **B** has two *meta*-aryl groups on the same side with two *ortho*-methyls of the imino aryl group. Pattern **C** has *meta*-aryl groups opposite *ortho*-methyls of the imino aryl group. Pattern **D** has two *meta*-aryls in one imino aryl group and two *ortho*-methyls in the second imino aryl group.

The Suzuki cross-coupling reaction offers a very convenient and reliable synthetic method for the introduction of a variety of aryl groups.[7] However, a preference was given to the aryl groups with electron-withdrawing substitutents, (e.g., 3,5-bis-(trifluoromethyl)phenyl and 4-fluorophenyl) because it has been shown that such groups can control polymer properties efficiently in Ni^{II} catalytic systems, even when placed relatively far from the catalytically active center.[8]

In this report, we describe the synthetic approach to the above complexes and their application as high-temperature catalysts for the production of α-olefins.

Results and Discussion

Synthesis. Complexes of type **A**, with four *meta*-aryl groups without *ortho*-methyls, were prepared by the following sequence. The condensation reaction between commercially available 1-(6-acetylpyridin-2-yl)ethanone (**2**) and 3,5-dibromo-4-methylphenylamine afforded bis(imino)pyridine **4** with four bromides in the *meta* positions of the aryl imino arms. The palladium-catalyzed Suzuki cross-coupling reaction between 4-fluorophenylboronic acid (**5**) and 2,6-bis(1-(3,5-dibromo-4-methyl)-phenylimino)ethyl)pyridine (**4**) was used to replace the four bromides with four aryls to form 2,6-bis(1-(3,5-di(4-fluorophenyl)-4-methyl)phenylimino)ethyl)pyridine (**9**) (Scheme 2). The

(4) (a) Bollmann, A.; Blann, K.; Dixon, J. T.; Hess, F. M.; Killian, E,; Maumela, H.; McGuinness, D. S.; Morgan, D. H.; Neveling, A.; Otto, S,; Overett, M.; Slawin, A. M. Z.; Wasserscheid, P.; Kuhlmann, S. *J Am. Chem. Soc*. **2004**, *126*, 14712. (b) Overett, M. J.; Blann, K.; Bollmann, A.; Dixon, J. T.; Haasbroek, D.; Killian, E.; Maumela, H.; McGuinness, D. S.; Morgan, D. H. *J Am. Chem. Soc.* **2005**, *127*, 10723.

(5) (a) Agarwal, R. K.; Chandra, A.; Fathima, P. A.; Shanti, T. R.; Hatha, A. A. M. *Pollut. Res.* **2005**, *24*, 247. (b) Frangi, C. *Tinctoria* **2002**, *99*, 26. (c) *National Emission Standards for Hazardous Air Pollutants: taconite iron ore processing*; Environmental Protection Agency, Emission Standards Div., U.S. EPA: Research Triangle Park, NC, 2003; Vol. 68, p 61868. (d) Buzard, G. S.; Kasprzak, K. S. *J. Environ. Pathol., Toxicol. Oncol.* **2000**, *19*, 179.

(6) (a) Schmid, M.; Eberhardt, R.; Klinga, M.; Leskela, M.; Rieger, B. *Organometallics* **2001**, *20*, 2321. (b) Moody, L. S.; MacKenzie, P. B.; Killian, C. M.; Lavoie, G. G.; Ponasik, J. A.; Smith, T. W.; Pearson, J. C.; Barrett, A. G. M. U.S. Pat. Appl. US 2002/0049135 A1. (c) Ionkin, A. S., Marshall, W. J. *Organometallics* **2004**, *23*, 3276.

(7) Miyaura, N.; Yanagi, T.; Suzuki, A. *Synth. Commun.* **1981**, *11*, 513.

(8) Zuideveld, M. A.; Wehrmann, P.; Rohr, C.; Mecking, S. *Angew. Chem., Int. Ed*. **2005**, *43*, 869.

Scheme 2. Synthesis of the Ligands 4 and 9 of Type A

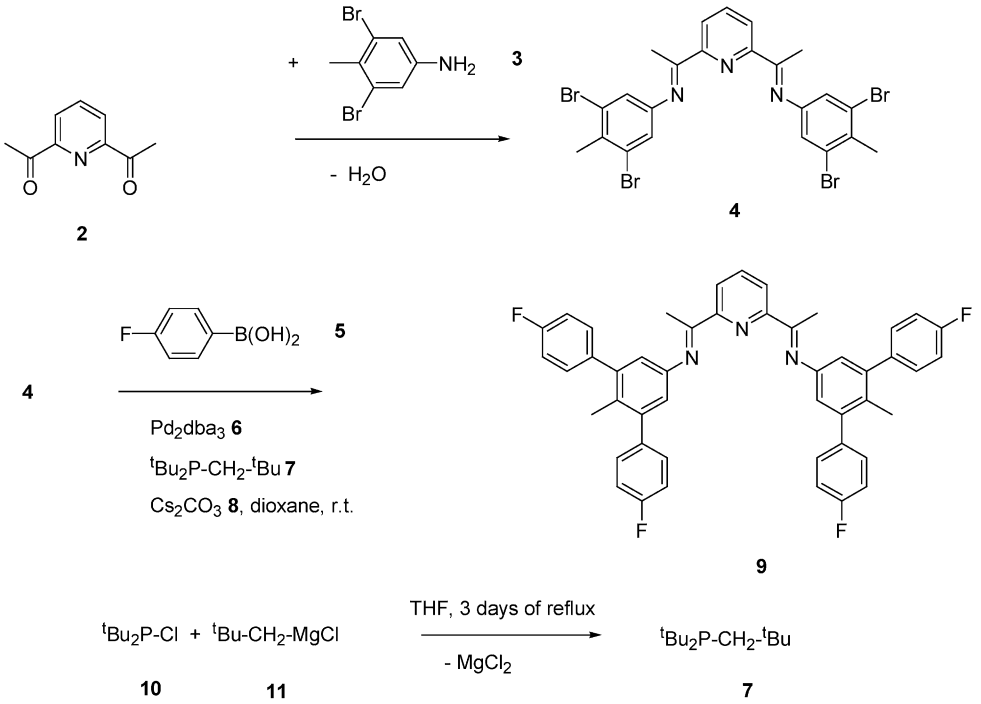

Scheme 3. Synthesis of Fe Complexes 12 and 13 of Type A

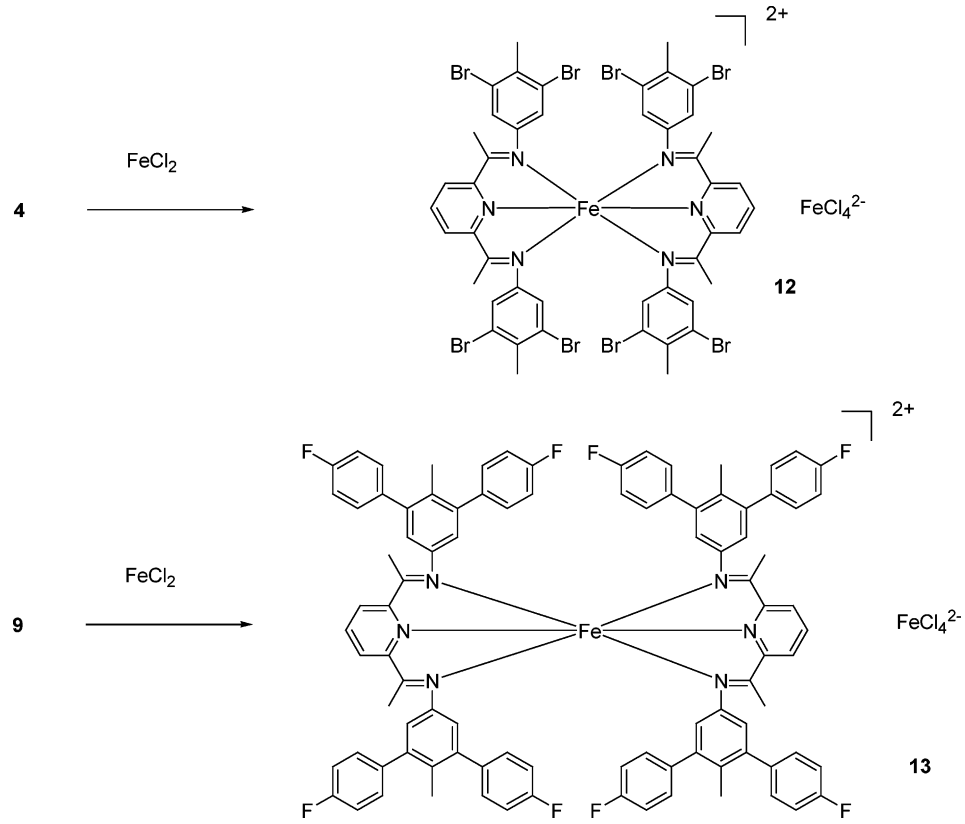

catalytic protocol involved Pd_2dba_3 (**6**)/di-*tert*-butyl-(2,2-dimethylpropyl)phosphane (**7**) as the catalyst in the presence of cesium carbonate with 1,4-dioxane as the solvent. Di-*tert*-butyl-(2,2-dimethylpropyl)phosphane (**7**) was synthesized by the prolonged refluxing of almost equimolar amounts of di-*tert*-butylchlorophosphine (**10**) and neopentylmagnesium chloride (**11**) in THF. Sterical bulky tertiary phosphines, such as **7**, bearing at least two *tert*-butyl groups, were found among the most efficient ligands for the palladium-catalyzed Suzuki cross-coupling reaction.[9]

Unexpectedly the coordination of Fe(II) chloride with ligands **4** and **9** resulted in the isolation of ion-paired complexes $[L_2Fe]^{2+}FeCl_4^{2-}$ **12** and **13** (Scheme 3).[10]

The structure of **13** was analyzed by X-ray analysis (Figure 1). The iron atom in the cation of complex **13** is octahedral, with six bonds to the imino nitrogens. Octahedral complex **13**

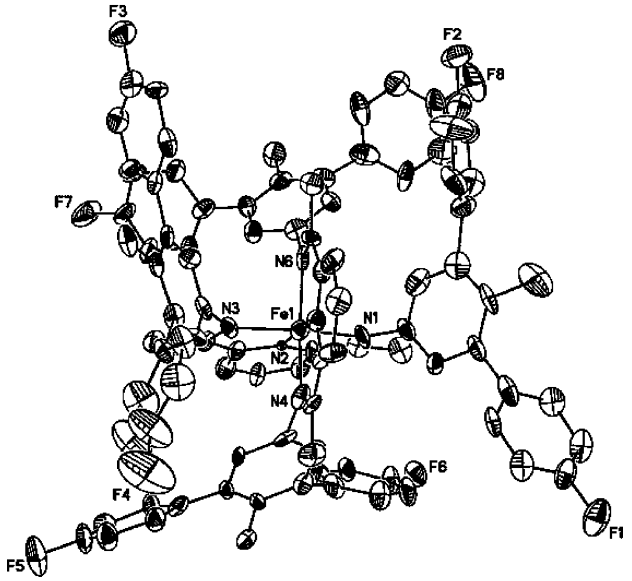

Figure 1. ORTEP drawing of the cationic part of iron(2^+), bis-[2,6-bis(1-(3,5-di(4-fluorophenyl)-4-methyl)phenylimino)ethyl)pyridine], tetrachloferrate(2^-) (**13**). Thermal ellipsoids are drawn to the 20% probability level. Hydrogen atoms are omitted for clarity.

has short Fe−N bonds varying from 1.84 to 1.98 Å. These are shorter by a maximum of 0.4 Å than all trigonal bipyramidal complexes in this study. Octahedral transition metal complexes having a d^4 to d^7 electronic configuration, like complex **13** with d^6 electronic configuration, possess mostly a low-spin electronic configuration.[11a,b] Pentacoordinated complexes, such as the trigonal bipyramidal complexes in this study, possess mostly a high-spin electronic configuration.[1d] According to ligand field theory,[11a,b] low-spin octahedral complexes always have shorter bonds by about 10% than high-spin complexes. This is exactly what is observed in the comparison of the bond lengths of octahedral **13** with the rest of the bipyramidal complexes in this article. These observations are consistent with other published data on iron octahedral complexes containing similar ligands.[11c]

The formation of the complexes **12** and **13** with a 1:2 ratio between metal and ligand can be explained by the lack of *ortho* substituents in ligands **4** and **9**. Apparently, the presence of even one methyl group in the *ortho* position of the imino aryl groups in bis(imino)pyridine ligands can stabilize the formation of 1:1 complexes (like complex **1**) with distorted bipyramidal geometry. These are coordinatively unsaturated and can be precatalysts for ethylene oligomerization. The complexes with octahedral geometry, like **13** with a 1:2 ratio, have a coordinatively saturated and sterically hindered iron atom, which should not afford an active site for ethylene oligomerization.

Complexes of type **B**, with two *meta*-aryl groups on the same side with two *ortho*-methyls of the imino aryl group, were synthesized by the following routes. Condensation between commercially available 1-(6-acetylpyridin-2-yl)ethanone (**2**) and 3-bromo-2-methylphenylamine (**14**) afforded 2,6-bis(1-(2-methyl-3-bromophenylimino)ethyl)pyridine (**15**) with two bromides in the *meta* positions of the aryl imino arms (Scheme 4). The palladium-catalyzed Suzuki cross-coupling reaction between 2,6-bis(1-(2-methyl-3-bromophenylimino)ethyl)pyridine (**15**) and 4-fluorophenylboronic acid (**5**), 3,5-bis(trifluoromethyl)phenylboronic acid (**16**), and 5-methyl-2-thiopheneboronic acid (**17**) afforded tridentate ligands **18**, **19**, and **20** of type **B**, correspondingly (Scheme 4). The same catalytic protocol was used as for the preparation of ligands **4** and **9** of type **A**.

Scheme 4. Synthesis of the Ligands 15 and 18−20 of Type B

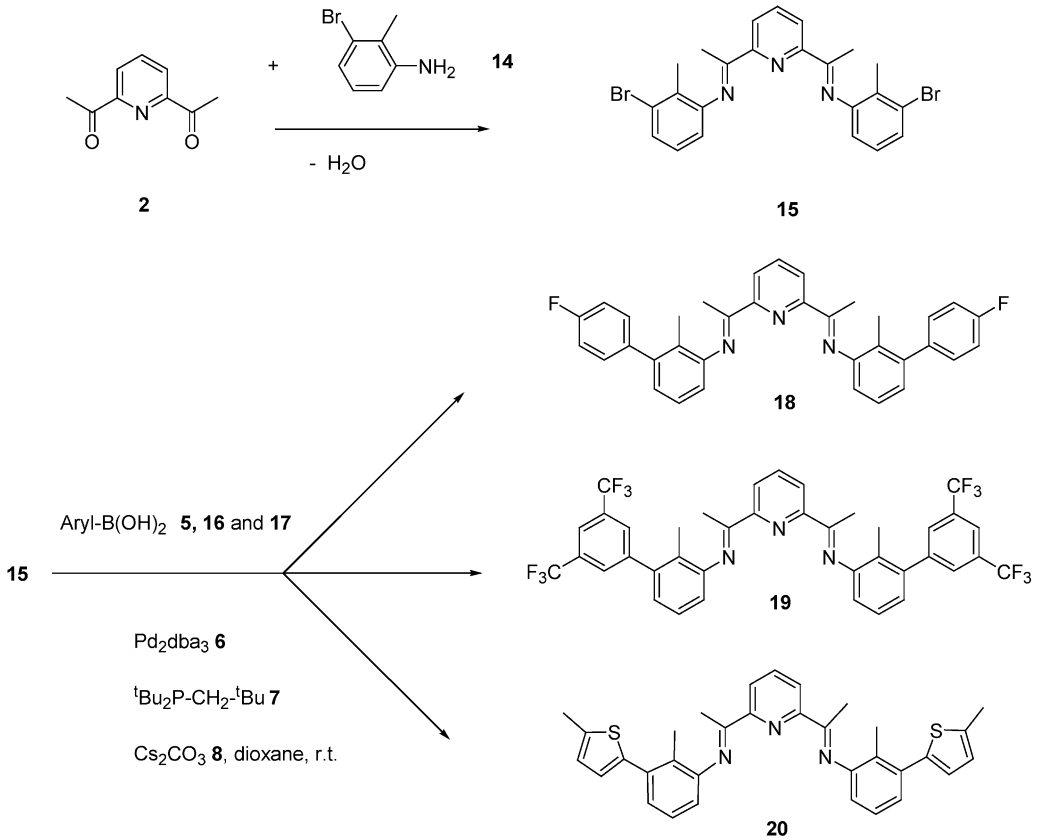

Scheme 5. Fe(II) Complexes 21−23 of Type B

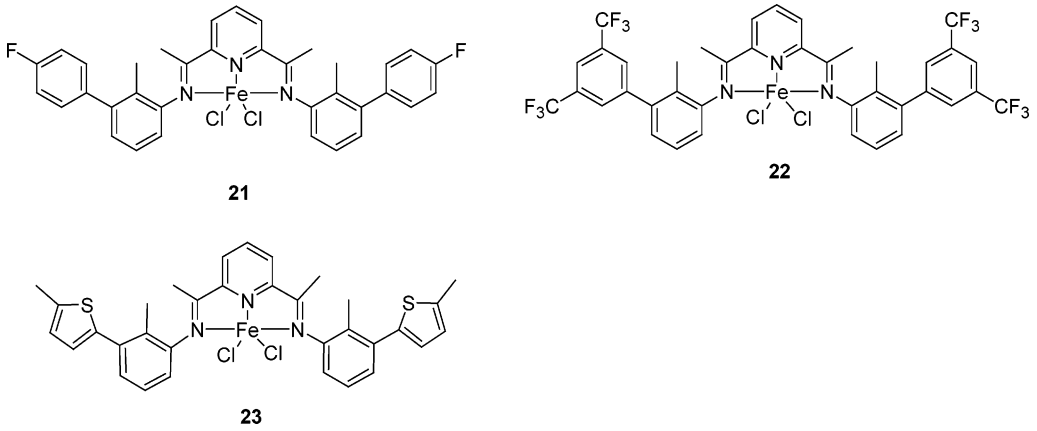

Scheme 6. Synthesis of Fe(II) Complex 22 and Fe(III) Complex 24 of Type B

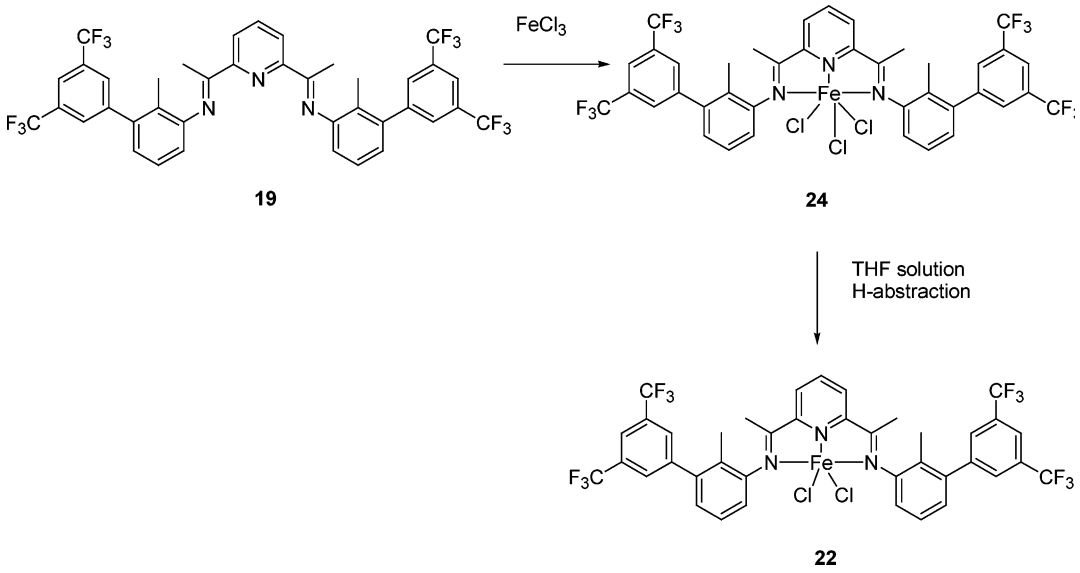

The Fe^{II} complexes **21**−**23** of type **B** were synthesized by the reaction of iron(II) chloride with ligands **18**−**20** in *n*-butanol or in THF (Scheme 5).

Complex **24**, with a trivalent iron center, was prepared by the reaction between iron(III) chloride and ligand **19** (Scheme 6). A crystal of **24** suitable for X-ray analysis was grown from benzene (Figure 2); this confirmed the trivalent state of iron and the tridentate mode of the coordination of ligand **19**.

The trivalent iron complex **24** was not stable in THF, undergoing reduction to become the divalent iron complex **22** within a week.[12] The reducing agent in this process is likely THF. Abstraction of hydrogen from THF has been found to be the cause of other such reductions.[13] A single crystal suitable for X-ray analysis of the material obtained from the reduction of **24** to **22** was grown from methylene chloride (Figure 3).

A type **C** complex, in which *meta*-aryl groups are opposite the *ortho*-methyls of the imino aryl group, was prepared by the sequence outlined below. The first reaction was the condensation between commercially available 1-(6-acetylpyridin-2-yl)ethanone (**2**) and 5-bromo-2-methylphenylamine (**25**) to yield 2,6-bis(1-(2-methyl-5-bromophenylimino)ethyl)pyridine (**26**). The palladium-catalyzed Suzuki cross-coupling reaction between compound **26** and 3,5-bis(trifluoromethyl)phenylboronic acid (**16**) afforded tridenate ligand **27** of type **C** (Scheme 7). A different catalytic protocol was used for the preparation of ligand **27**. Benzyldi-*tert*-butylphosphane (**28**) was employed instead of di-*tert*-butyl(2,2-dimethylpropyl)phosphane (**7**) in the cross-coupling reaction. The sterically bulky phosphane **28** was obtained by prolonged refluxing of almost equimolar amounts of di-*tert*-butylchlorophosphine (**10**) and of benzylmagnesium chloride (**29**) in THF.[14]

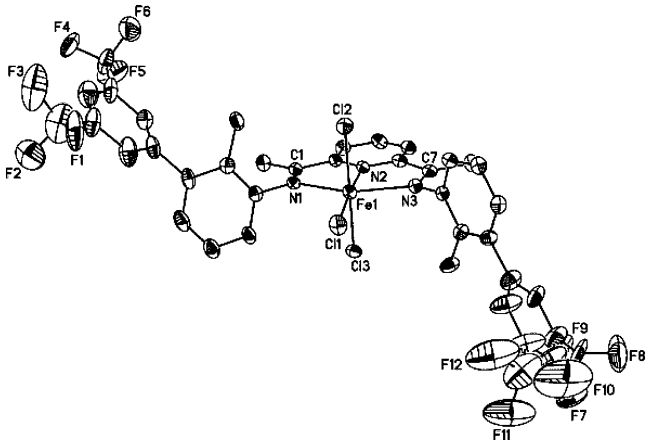

Figure 2. ORTEP drawing of 2,6-bis(1-(2-methyl-3-(3,5-bis(trifluoromethyl)phenyl)phenylimino)ethyl)pyridineiron(III) chloride (**24**). Thermal ellipsoids are drawn to the 20% probability level. Some CF_3 groups were split into six fluorine positions due to disorder. Only three fluorine positions on each CF_3 group are depicted, and all hydrogen atoms are omitted for clarity.

Scheme 7. Synthesis of Fe Complex 30 of Type C

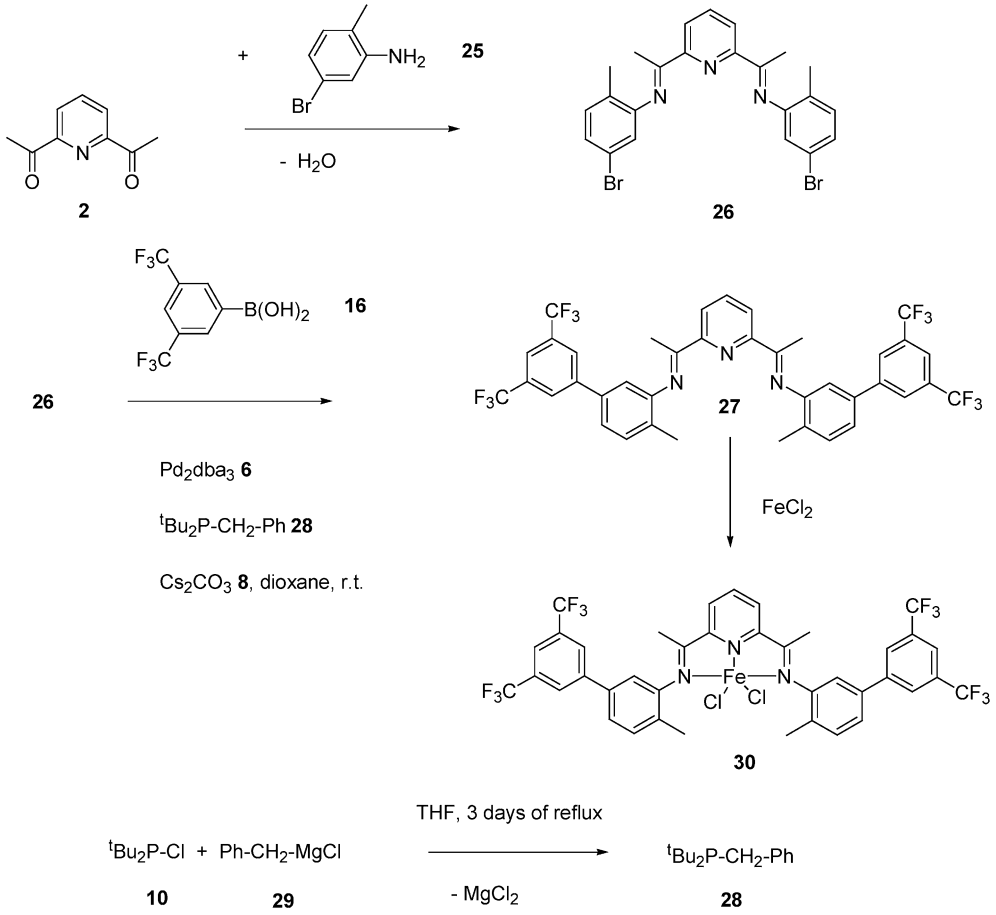

The reaction of iron(II) chloride with ligand **27** afforded complex **30** of type **C**. A crystal of **30** suitable for X-ray was grown from pentane (Figure 4).

A complex of type **D**, in which two *meta*-aryls in one imino aryl group and two *ortho*-methyls in the second imino aryl group, was synthesized by the following reaction sequence. Two successive condensations, the first between 2,6-diacetylpyridine and 4-bromo-2,6-dimethylphenylamine yielding compound **31**, followed by a second condensation with 3,5-dibromo-4-methylphenylamine (**3**), were used to prepare nonsymmetrical ligand **32**. Suzuki cross-coupling between bis(imino)pyridine **15** with three bromides and 3,5-bis(trifluoromethyl)phenylboronic acid (**16**) afforded tridentate ligand **33** of type **D** (Scheme 8). The

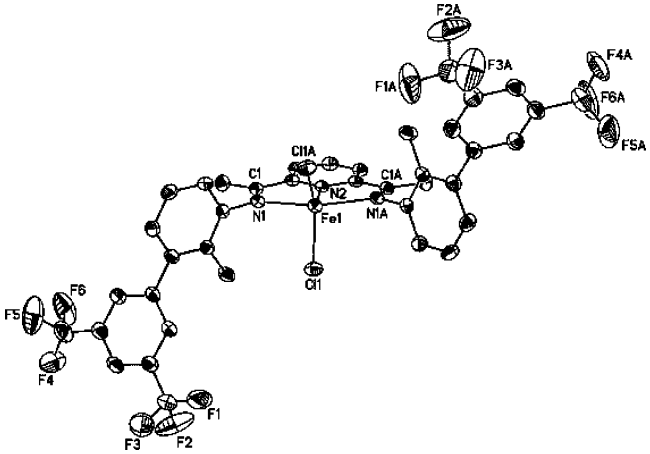

Figure 3. ORTEP drawing of 2,6-bis(1-(2-methyl-3-(3,5-bis-(trifluoromethyl)phenyl)phenylimino)ethyl)pyridineiron(II) chloride (**22**). Thermal ellipsoids are drawn to the 50% probability level. Some CF_3 groups were split into six fluorine positions due to disorder. Only three fluorine positions on each CF_3 group are depicted, and all hydrogen atoms are omitted for clarity.

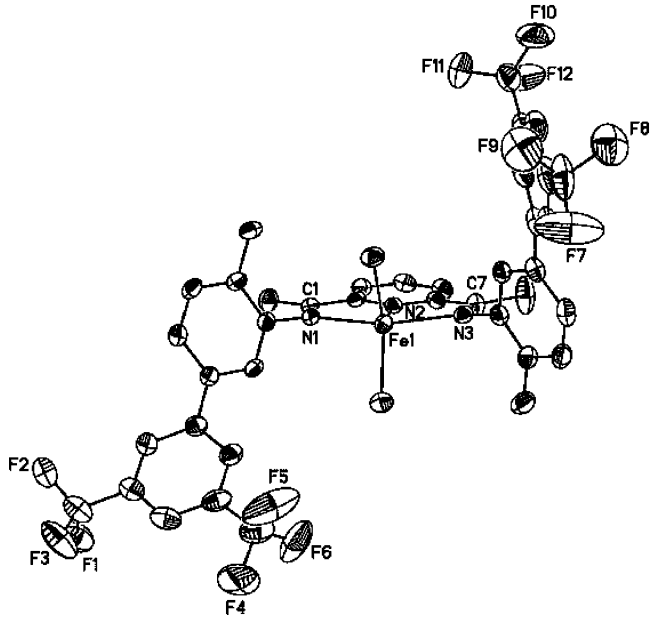

Figure 4. ORTEP drawing of 2,6-bis(1-(2-methyl-5-(3,5-bis-(trifluoromethyl)phenyl)phenylimino)ethyl)pyridineiron(II) chloride (**30**). Thermal ellipsoids are drawn to the 50% probability level. Some CF_3 groups were split into six fluorine positions due to disorder. Only three fluorine positions on each CF_3 group are depicted, and all hydrogen atoms are omitted for clarity.

Scheme 8. Synthesis of Fe Complex 34 of Type D

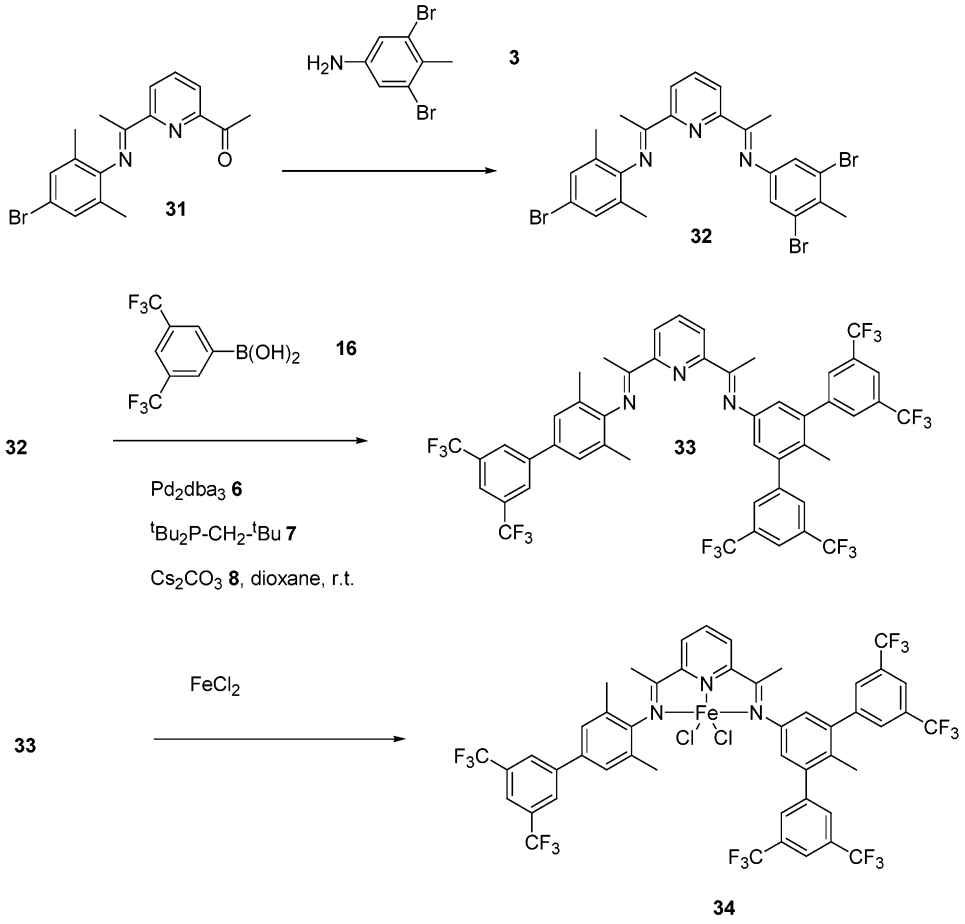

same catalytic protocol was used as for the preparation of ligands of types **A** and **B**. The reaction between ligand **33** and iron(II) chloride in THF afforded complex **34** of type **D**.

The structure of complex **34** is shown in Figure 5. A crystal of **34** suitable for X-ray analysis was grown from methylene chloride.

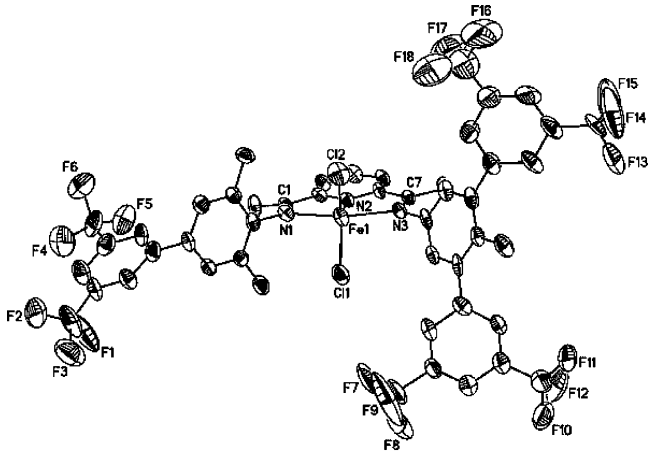

Figure 5. ORTEP drawing of 4-(3,5-bis(trifluoromethyl)phenyl)-2,6-dimethylphenyl)-(1-{6-[1-(3,5-(3,5-bis(trifluoromethyl)phenyl)-4-methylphenylimino)ethyl]pyridin-2-yl}ethylidene)amineiron(II) chloride (**34**). Thermal ellipsoids are drawn to the 50% probability level. Some CF_3 groups were split into six fluorine positions due to disorder. Only three fluorine positions on each CF_3 group are depicted, and all hydrogen atoms are omitted for clarity.

Solid-State Structures of Fe Precatalysts. Complexes **22**, **30**, and **34** have distorted bipyramidal geometries, which are typical for iron(II) complexes with tridentate bis(imino)pyridine ligands in a ratio of 1:1.[15] The planes of the *ortho*-methyl-*meta*-aryl-substituted arylimino groups of complexes **22** and **30** are oriented orthogonally to the plane formed by iron and the three nitrogen atoms. *ortho*-Methyl-*meta*-aryl-substituted groups are oriented in "up−down" conformation relative to each other in the solid state for **22** and **30**. Unexpectedly, complex **1** was found mostly in the "up−up" conformation, with only 28% of the symmetrical up−down conformation. One might expect that the symmetrical "up−down" conformer would be predominant in all cases. This is evidence that rotation of the aryl group

(9) Christmann, U.; Vilar, R. *Angew. Chem., Int. Ed.* **2005**, *44*, 366.

(10) Chen, Y.; Qian, C.; Sun, J. *Organometallics* **2003**, *22*, 1236.

(11) (a) Hauser, A. *Top. Curr. Chem.* **2004**, *233*, 49. (b) Hauser, A.; Jeftic, J.; Romstedt, H.; Hinek, R.; Spiering, H. *Coord. Chem. Rev.* **1999**, *190−192*, 471. (c) Scheer, C.; Chautemps, P.; Gautier-Luneau, I.; Pierre, J.; Serratrice, G. *Polyhedron* **1996**, *15*, 219.

(12) Bryliakov, K. P.; Semikolenova, N. V.; Zudin, V. N.; Zakharov, V. A.; Talsi, E. P. *Catal. Commun.* **2004**, *5*, 45.

(13) (a) Moreira, R. F.; Tshuva, E. Y.; Lippard, S. J. *Inorg. Chem.* **2004**, *43*, 4427. (b) Li, R.; Smith, R. L.; Kenttamaa, H. I. *J. Am. Chem. Soc.* **1996**, *118*, 5056. (c) Malatesta, V.; Ingold, K. U. *J. Am. Chem. Soc.* **1981**, *103*, 609.

(14) (a) Johnson, L. K.; McLain, S. J.; Sweetman, K. J.; Wang, Y.; Bennett, A. M. A.; Wang, L.; McCord, E. F.; Ionkin, A.; Ittel, S. D.; Radzewich, C. E.; Schiffino, R. S. PCT Int. Appl. WO 2003044066 A2, 2003; 170 pp. (b) Stauffer, S. R.; Hartwig, J. F. *J. Am. Chem. Soc.* **2003**, *125*, 6977. (c) Stewart, A. P.; Trippett, S. *J. Chem. Soc. C* **1970**, *9*, 1263.

(15) (a) Britovsek, G. J. P.; Mastroianni, S.; Solan, G. A.; Baugh, S. P. D.; Redshaw, C.; Gibson, V. C.; White, A. J. P.; Williams, D. J.; Elsegood, M. R. J. *Chem. Eur. J.* **2000**, *6*, 2221. (b) Bianchini, C.; Mantovani, G.; Meli, A.; Migliacci, F.; Zanobini, F.; Laschi, F.; Sommazzi, A. *Eur. J. Inorg. Chem.* **2003**, *8*, 1620.

Table 1. Selected Bond Lengths (Å) and Conformer's Ratio for 1, 22, 24, 30, 34, and 15

	1	22	24	30	34	15
axial (imino) N−Fe bond	2.2303(16) Fe−N1	2.221(2) Fe−N1	2.190(4) Fe−N3	2.231(2) Fe−N1	2.209(9) Fe−N3	N/A
axial (imino) N−Fe bond	2.2424(17) Fe−N3	2.221(2) Fe−N1A	2.193(4) Fe−N1	2.241(2) Fe−N3	2.260(9) Fe−N1	N/A
basal (central) N−Fe bond	2.0943(16) Fe−N2	2.133(3) Fe−N2	2.121(4) Fe−N2	2.107(2) Fe−N2	2.096(9) Fe−N2	N/A
C═N	1.281(2) N1−C1	1.284(3) N1−C1	1.260(7) N1−C1	1.288(3) N1−C1	1.283(13) N1−C1	1.294(9) N2−C6
C═N	1.287(3) N3−C7	1.284(3) N3−C7	1.271(7) N3−C7	1.277(3) N3−C7	1.270(13) N3−C7	1.286(8) N3−C23
ratio of up−up to up−down isomers	72% of up−up and 28% of up−down	up−down	up−down	up−down	N/A	up−up

around the C−N bonds does take place, and this must be considered in the interpretation of oligomerization results.

The introduction of additional aryl substituents in the *meta* positions next to the *ortho*-methyls (type **B**, complex **22**) resulted in a shortening of the axial Fe−N bonds by 0.0093 and 0.0214 Å relative to the parent complex **1** (Table 1). This shortening of Fe−N bonds was not observed in the case of complex **30**, with aryl substituents in 3,5-*ortho*-*meta*-substitution (type **C**). The axial Fe−N bond lengths for **1** and **30** are essentially identical. The bond lengths of the imino groups of ligand **15** and its Fe complex **22** are also identical within experimental error. The bond lengths of the imino moieties of ligand **15** did not undergo a significant change upon the formation of its Fe complex **22**. Both of them have a typical C═N double bond length around 1.28 Å.[16]

Nonsymmetrical complex **34** has the longest and the shortest axial N−Fe bonds among distorted bipyramidal structures in this study. The longest [2.260(9) Å] is the bond of the moiety with two *ortho*-methyl groups. The steric repulsive interaction between the *ortho*-methyl groups and the iron core of the molecule is likely responsible for this elongation. The moiety without *ortho*-methyl groups in **34** has the shortest N−Fe distance at 2.209(9) Å. *meta*-Aryl groups in **34** are rotated away from the main plane of the iminophenyl group with angles ranging from 35.4° to 59.1°.

The geometry of the six-coordinated iron atom in the trivalent complex **24** may be described as distorted-octahedral. The axial N−Fe bonds in **24** are shorter by 0.031 Å than corresponding bonds in the divalent complex **22**, reflecting the effects of the higher oxidation state of the iron in **24**.

Oligomerization of Ethylene to α-Olefins by Iron Complexes 1, 21, 22, 23, 24, 30, and 34. Oligomerizations were run at 700 psig of ethylene in *o*-xylene at 120 and 130 °C. The resulting product mixtures were evaluated for soluble α-olefins via GC and for insolubles via a filtration/gravimetric method. The distribution of soluble α-olefins and the percent solids of total α-olefins are important factors for the evaluation of a potential catalyst. A product distribution, which fits the theoretical Shultz−Flory distribution, is optimal to minimize ethylene yield loss. α-Olefins of carbon number greater than 40 make up the percent solids of total α-olefins. Values for these below that predicted by the Shultz−Flory distribution were desired. As noted above, C_6 to C_{16} α-olefins are targeted for a general commercial application.

Another important factor is the catalyst productivity measured as kg α-olefins/g catalyst. This is a function of the catalyst/ethylene kinetics and catalyst thermal stability. An indication of the thermal stabilities, lifetimes at a given temperature, was obtained by measuring the periods of time over which oligomerizations consumed ethylene. The validity of such comparisons is a function of the amount of catalyst injected. If too much is added, a large exotherm will result, and the catalyst is overheated and so decomposes more rapidly to give a shorter uptake time. With too small of an amount, the uptake will fall below the ethylene flowmeter detection limit, and so again an underestimate of uptake time will result. To address this problem, the amounts of catalysts added were adjusted such that the batch temperature stayed within 2 °C of the set point. While this meant there could be a large range of catalyst charges, similar amounts of α-olefins were made for all runs and the ethylene uptake times were a valid measure of the catalyst lifetimes. In addition, the α-olefin analytical methods were applied over a comparable concentration range, which is desirable. A table of lifetime results is shown in Table 2.

Table 2. Estimates of Lifetimes of Catalysts from Ethylene Uptake at 120 °C and 700 psig

	precatalyst						
	1	**21**	**22**	**23**	**24**	**30**	**34**
lifetime (min)	2.9	20.0	11.5	20.0	11.2	16.7	20.0

Before considering data trends with respect to precatalyst structure, the main focus is to compare the parent methyl-substituted Fe^{II} complex **1** to all of the other precatalysts with greater degrees of substitution (types **B**−**D**).

With respect to the lifetime data in Table 2, it is seen that the parent methyl-substituted Fe^{II} complex **1** has by far the shortest lifetime. Otherwise, it appears that having the *meta* 3,5-bis(trifluoromethyl)phenyl group on the same side with the *ortho*-methyl in **22** of type **B** gives a shorter lifetime versus when the *meta* 3,5-bis(trifluoromethyl)phenyl group is on the side opposite the *ortho*-methyl of the imino aryl group, such as in complex **30** of type **C**. Also, the iron oxidation state (**22** vs **24**) appears to have no effect on lifetime.

A list of precatalyst productivities is in Table 3. The precatalysts with patterns of double substitution tend to last longer after an initial uptake but give substantially lower conversions of ethylene. The parent methyl-substituted Fe^{II} complex **1** is by far the most productive. It is followed by precatalyst **30** of type **C** and by precatalyst **34** of type **D**. All other precatalysts have about the same productivities. This seems to indicate that bulky groups in the *ortho* positions slow access of ethylene to the metal center of the catalyst.

While most of the precatalysts have half the productivity of precatalyst **1**, they are nonetheless useful: all of these catalysts are highly productive by α-olefins industry standards, and the amounts needed are insignificant in terms of α-olefin production costs. As was mentioned earlier, with a shorter lifetime in a continuous plug-flow process, there would be a need to install and maintain more injection points, which could add significant initial investment and production costs. This means precatalyst

(16) De Bruin, B.; Bill, E.; Bothe, E.; Weyhermueller, T.; Wieghardt, K. *Inorg. Chem.* **2000**, *39*, 2936.

Table 3. α-Olefins from Ethylene Oligomerizations by Iron Complexes 1, 21, 22, 23, 24, and 30[a]

entry	precatalyst/ amount μmol	amount cocatalyst, MMAO, mmol	temperature, °C	"*K*" value Shultz−Flory distribution[b]	kg of LAO per g of catalyst	% solids total LAO [c]	SFD R^2
1	**21**/0.457	2.26	130	0.68	125	7.83	0.9628
2	**21**/0.610	1.13	120	0.68	54	8.89	0.9923
3	**22**/0.336	2.26	130	0.67	124	5.10	0.9901
4	**22**/0.224	2.26	120	0.69	123	3.66	0.9781
5	**22**/0.090	0.68	120	0.67	160	7.37	0.9920
6	**23**/0.121	1.13	120	0.68	142	8.81	0.9882
7	**24**/0.107	1.13	120	0.64	128	7.56	0.9968
8	**24**/0.053	1.13	120	0.65	128	9.48	0.9968
9	**30**/0.112	1.13	120	0.57	249	4.39	0.9906
10	**34**/0.08	1.13	120	0.70	197	4.55	0.9969
11	**1**/0.064	1.13	120	0.59	458	3.44	0.9862

[a] Conditions: solvent: xylenes; pressure: 700 psig. [b] Determined from GC, using extrapolated values for C-10 and C-12. [c] Xylenes-insoluble fraction of α-olefins.

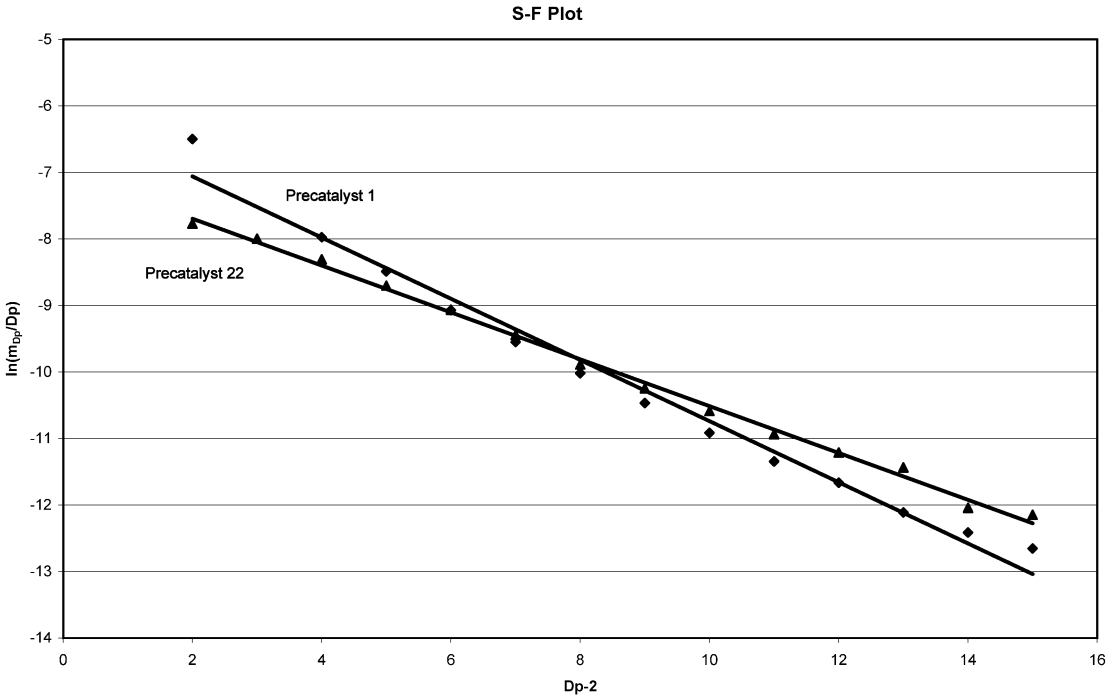

Figure 6. Distribution of α-olefins from C-2 to C-14 for precatalysts **1** (squares) and precatalyst **22** (triangles).

21, **23**, or **34** may be a better choice than **1** with regard to productivity/lifetime considerations.

The ion-pared complex $[L_2Fe]^{2+}FeCl_4^{2-}$ **13** of type **A** was found to be inactive in α-olefin oligomerization experiments within the tested temperature range of 100−130 °C.

The desired α-olefin product distribution depends on the targeted application. For this work, a *K* factor in the range 0.6 to 0.7 was desired. The distribution obtained depends on the propagation and termination rates associated with a given catalyst. An olefin growth factor *K* is defined by the equation

$$K = R_p/(R_p + R_t)$$

where R_P is the rate of propagation and R_t is the rate of termination. This growth factor is used in the following form of the Schulz−Flory distribution equation:[17]

$$\ln(m_p/D_p) = \ln((1 - K)\wedge 2/(2 - K)) + (D_p - 2)\ln K$$

where m_p is the weight fraction of the α-olefin and D_p is the degree of polymerization of the α-olefin

If the catalyst makes a Shultz−Flory distribution of α-olefins, a plot of $\ln(m_p/D_p)$ versus $(D_p - 2)$ should give a linear relationship with the slope equal to the inverse logarithm of the growth factor *K*. An example of such a plot is shown in Figure 6. The low and high ends of the distribution for precatalyst **1** deviate more from the line than do those for precatalyst **22**. The low and high end products are of less commercial value, so the deviations by the parent methyl-substituted Fe^{II} complex **1** yield a less desirable product mix.

The linear regression coefficients (R^2) for such plots are indicators of the distribution ideality. The closer the value is to 1, the more ideal is the product distribution. The right-hand column in Table 3 contains a list of R^2 values. A ranking of R^2 values from high to low indicates that precatalyst **1** falls near the bottom of the list. The nonsymmetric precatalyst **34** is at the top. Precatalysts **22** and **30**, with their different substitution patterns of the same 3,5-bis(trifluoromethyl)phenyl groups, have nearly the same value.

Growth factors (*K*) for the precatalysts are also listed in Table 3. Considering the categories mentioned above, the parent

(17) Elvers, B., et al., Eds. In *Ullmann's Encyclopedia of Industrial Chemistry*; VCH Verlagsgesellschaftmbh: Weinheim, 1989; Vol. A13, pp 243−247 and 275−276.

methyl-substituted Fe(II) complex **1** has close to the lowest *K* value. This suggests that the multiple substitutions for the others raise the distributions, meaning that they make, on average, longer α-olefins. The highest value was obtained by nonsymmetrical precatalyst **34** of type **D**. Reaching *K*'s in the 0.65−0.70 range at temperatures of 120−130 °C is advantageous because a desirable product distribution is made over a temperature range where olefin solubility is enhanced to reduce reactor fouling.

The values for percent solids of total α-olefins are also listed in Table 3. In a rank of lowest to highest, precatalyst **1** yields the lowest solids. Precatalysts **22** and **30** have similar values, suggesting location of the same 3,5-bis(trifluoromethyl)phenyl groups in different positions had no detectable effect. Nonsymmetric precatalyst **34** ranks near the top of the list. It should be kept in mind that the measurements of percent solids are not as precise as, for example, *K* values or productivities. Thus, the data for percent solids are slightly scattered.

From the data in Table 3, it is seen that precatalysts with double patterns of substitutions have lower productivities, higher *K* values, and higher percent solids of total α-olefins. Hindered ethylene access to the reaction center was proposed earlier as the explanation of reduced catalytic activity of the bulkier iron tridentate catalysts.[1c] Theoretical calculations later confirmed that ethylene capture is the rate-determining step in these oligomerizations.[19] On the other hand, increasing the steric bulk above and below the planes of iron and nickel in the Versipol family of catalysts has been shown to slow chain transfer relative to chain propagation.[1] This, in turn, should lead to the higher growth factors and higher percent solids of total α-olefins (LAO) for the precatalysts with double patterns of substitutions. The higher percent solids of total LAO made for these catalysts, also seen in Table 3, would support this proposal. As the distributions are shifted to higher MW products, more insolubles are made. The losses in productivities are real because the solids were included in the productivity calculations. In addition, the double-substituted catalysts have longer lifetimes than precatalyst **1**, but their productivities are much lower. It appears then that the bulky second substitutions affected the propagation rates. Precatalysts **22** and **30** have two large 3,5-electron-withdrawing bis(trifluoromethyl)phenyl groups on the imino aryls, but the productivities of **22** versus **30** are very different. This would suggest that the locations of the bulky groups make the difference. In **22**, the bulky bis(trifluoromethyl)phenyl groups are adjacent to the *ortho*-methyl, but in **30** they are opposite. The latter could give more ready access to the metal center for ethylene addition and chain transfer. Precatalyst **34** has a productivity that falls between **22** and **30**. Again, the substitution pattern is very different. The issue is whether this is a predominantly steric or electronic effect. Precatalysts **21** and **23** have aromatic groups with somewhat different electron-withdrawing ability and with approximately the same bulk at the same *meta* positions as **22**, but their *K* values and productivities are all nearly the same. This would suggest that the electron-withdrawing effects are minimal and that the substitution pattern matters most.

Typical qualities of α-olefins prepared by the Versipol catalysts with double patterns of substitutions are shown in Table 4. They are in line with previously reported numbers.[1c,e] The amount of undesirable branched olefins are below 2 wt %, and the amounts of internal olefins are below the 2500 ppm level. The purity range slightly exceeds the range reported for the SHOP process.[2b] Detailed purity analysis and further comparisons with current α-olefins processes are outside the scope of this study.

Table 4. Typical Quality of α-Olefins and Impurities from the Oligomerization Experiments of the Fe^{II} Tridentate Catalysts with Double Patterns of Substitution

product	LAO, wt %	internal olefins, ppm	branched olefins, wt %
C4	99.98	215	
C6	99.24	1128	0.64
C8	98.36	2325	1.41
C10	97.61	2210	2.17

As was found by X-ray analysis for the solid state, the precatalyst **1** forms two conformers: an "up and down" conformer and an "up−up conformer" (Scheme 9). It is reasonable to suggest the existence of those conformers in the solution during the oligomerization. The "up and down" conformer offers symmetrical steric protection of both axial sides of iron (below and above the N−Fe(N)−N plane). The "up and up" conformer protects one axial side only by two *ortho*-methyl groups, leaving the other side unprotected. If oligomerization of ethylene commences from the side protected by two methyl groups, it should lead to a heavier fraction of α-olefins. If the oligomerization of ethylene commences from the unprotected side of the conformer, it should lead to a light fraction of α-olefins. According to theoretical calculations of the polymerization mechanisms on Fe^{II} catalysts with tridentate bis(imino)pyridine ligands, the chain propagation takes place from the same axial side of the N−Fe(N)−N plane with backside approach of ethylene to the alkyl chain.[19] As a result, the "up and up" conformer of **1** will contribute to curvature of the Shultz−Flory distribution of α-olefins, while the symmetrical "up and down" conformer should obey the Shultz−Flory distribution. The possibility of different "interconverting isomers" in a family of nonsymmetrical iron tridentate catalysts has been proposed in the case of propylene polymerization.[20]

The importance of the conformeric behavior of these complexes with regards to the steric protection of the axial sides of the iron center is clear upon comparisons of oligomerization results of precatalysts **22** and **30**, which are isomers. Both of them have the same electron-withdrawing 3,5-bis(trifluoromethyl)phenyl group in *meta* positions (Scheme 9). However there is substantial differences in the catalytic performance. The precatalyst **30** behaves as catalyst **1**, giving substantial deviation from the Shultz−Flory distribution, low *K* value, and very good productivity (Table 2). Precatalyst **22** afforded α-olefins with more ideal Shultz−Flory distribution, higher *K* value, and reduced productivity. Thus, steric factors appear to be more important than electronic ones. Precatalyst **22** likely exists mostly as an "up and down" conformer in solution, in which the additional 3,5-bis(trifluoromethyl)phenyl groups in the *meta* positions from the same side of the *ortho*-methyls keep the arylimino groups in an up and down conformation and restrict 180° rotation of the aryl groups around the C−N bonds. The conformational behavior of **30** closely resembles that of **1**, and additional increase of steric bulk in **30** resulted in lower productivity.

Precatalyst **34** has two *ortho*-methyl groups closely protecting both axial sides of iron from one side and two aryl groups in *meta* positions protecting the axial sides remotely. It appears that this combination of steric protection is the best with regard

(18) Bart, S. C.; Lobkovsky, E.; Chirik, P. J. *J. Am. Chem. Soc.* **2004**, *126*, 13794.

(19) (a) Deng, L.; Margl, P.; Ziegler, T. *J. Am. Chem. Soc.* **1999**, *121*, 6479. (b) Ramos, J.; Cruz, V.; Munos-Escalona, A.; Martinez-Salazar, J. *Polymer* **2002**, *43*, 3635.

(20) Small, B. L.; Brookhart, M. *Macromolecules* **1999**, *32*, 2120.

Table 5. Summary of Crystal Data, Data Collection, and Structural Refinement Parameters for 1, 13, 15, and 22

	1	13	15	22
empirical formula	$C_{24}H_{25}Cl_4FeN_3$	$C_{94}H_{70}Cl_4F_8Fe_2N_6$	$C_{39}H_{27}F_{12}N_3$	$C_{41}H_{31}Cl_6F_{12}FeN_3$
FW	553.12	1689.06	765.64	1062.24
cryst color, form	blue, needle	black, block	colorless, block	green, plate
cryst syst	monoclinic	orthorhombic	orthorhombic	monoclinic
space group	*P*2(1)/*c*	*P*2(1)2(1)2	*Pna*2(1)	*C*2/*c*
a (Å)	10.4140(5)	13.482(5)	16.770(2)	11.5071(4)
b (Å)	15.2465(8)	23.751(8)	15.807(2)	12.4346(5)
c (Å)	15.8488(8)	26.066(11)	27.350(4)	31.4986(13)
α (deg)	90	90	90	90
β (deg)	92.3650(10)	90	90	100.3450(10
γ (deg)	90	90	90	90
V (Å^3)	2514.3(2)	8347(5)	7250.0(16)	4433.7(3)
Z	4	4	8	4
density (g/cm^3)	1.461	1.344	1.403	1.591
abs *μ* (mm^{-1})	1.042	0.544	0.126	0.787
F(000)	1136	3472	3120	2136
cryst size (mm)	0.32 × 0.06 × 0.02	0.12 × 0.12 × 0.06	0.28 × 0.14 × 0.12	0.34 × 0.32 × 0.07
temp (°C)	−100	−100	−100	−100
scan mode	*ω*	*ω*	*ω*	*ω*
detector	Bruker-CCD	Bruker-CCD	Bruker-CCD	Bruker-CCD
θ_{max} (deg)	27.96	22.08	28.35	28.46
no. obsvd reflns	37 670	23 505	45 419	23 576
no. uniq reflns	6038	10 182	14 682	5577
R_{merge}	0.0547	0.1818	0.1477	0.0356
no. params	358	1031	981	298
S[a]	1.02	0.924	0.968	1.039
R indices [$I > 2\sigma(I)$][b]	$wR_2 = 0.075$, $R_1 = 0.037$	$wR_2 = 0.220$, $R_1 = 0.099$	$wR_2 = 0.153$, $R_1 = 0.076$	$wR_2 = 0.131$, $R_1 = 0.051$
R indices (all data)[b]	$wR_2 = 0.084$, $R_1 = 0.060$	$wR_2 = 0.302$, $R_1 = 0.231$	$wR_2 = 0.223$, $R_1 = 0.251$	$wR_2 = 0.142$, $R_1 = 0.068$
max. diff peak, hole (e/Å^3)	0.288, −0.325	0.610, −0.549	0.395, −0.348	0.956, −0.553

[a] GooF $= S = \{\sum[w(F_o^2 - F_c^2)^2]/(n - p)\}^{1/2}$, where *n* is the number of reflections, and *p* is the total number of refined parameters. [b] $R_1 = \sum||F_o| - |F_c||/\sum|F_o|$, $wR_2 = \{\sum[w(F_o^2 - F_c^2)^2]/\sum[w(F_o^2)^2]\}^{1/2}$ (sometimes denoted as R_w^2).

Table 6. Summary of Crystal Data, Data Collection, and Structural Refinement Parameters for 24, 30, and 34

	24	30	34
empirical formula	$C_{51}H_{39}Cl_3F_{12}FeN_3$	$C_{39}H_{27}Cl_2F_{12}FeN_3$	$C_{102}H_{74}Cl_{16}F_{36}Fe_2N_6$
fw	1084.05	892.39	2746.57
cryst color, form	gold, plate	blue, needle	blue, needle
cryst syst	monoclinic	monoclinic	monoclinic
space group	*P*2(1)	*C*2/*c*	*P*2(1)/*c*
a (Å)	16.000(2)	32.663(4)	20.024(11)
b (Å)	19.310(3)	15.197(2)	21.142(12)
c (Å)	16.689(3)	15.494(2)	29.448(18)
α (deg)	90	90	90
β (deg)	90.168(3)	96.197(2)	105.241(14)
γ (deg)	90	90	90
V (Å^3)	5156.2(14)	7646.0(17)	12028(12)
Z	4	8	4
density (g/cm3)	1.396	1.55	1.517
abs *μ* (mm^{-1})	0.528	0.627	0.699
F(000)	2204	3600	5504
cryst size (mm)	0.21 × 0.09 × 0.03	0.420 × 0.080 × 0.030	0.85 × 0.08 × 0.02
temp (°C)	−100	−100	−100
scan mode	*ω*	*ω*	*ω*
detector	Bruker-CCD	Bruker-CCD	Bruker-CCD
θ_{max} (deg)	26.45	29.35	24.34
no. obsvd reflns	43 238	23 662	54 411
no. uniq reflns	10 557	23 680	17 640
R_{merge}	0.1054	0	0.1494
no. params	553	539	1469
S[a]	0.92	0.944	1.417
R indices [$I > 2\sigma(I)$][b]	$wR_2 = 0.223$, $R_1 = 0.084$	$wR_2 = 0.196$, $R_1 = 0.080$	$wR_2 = 0.309$, $R_1 = 0.132$
R indices (all data)[b]	$wR_2 = 0.261$, $R_1 = 0.172$	$wR_2 = 0.233$, $R_1 = 0.144$	$wR_2 = 0.346$, $R_1 = 0.218$
max. diff peak, hole (e/Å^3)	0.538, −0.451	1.371, −0.737	3.611, −0.936

[a] GooF $= S = \{\sum[w(F_o^2 - F_c^2)^2]/(n - p)\}^{1/2}$, where *n* is the number of reflections, and *p* is the total number of refined parameters. [b] $R_1 = \sum||F_o| - |F_c||/\sum|F_o|$, $wR_2 = \{\sum[w(F_o^2 - F_c^2)^2]/\sum[w(F_o^2)^2]\}^{1/2}$ (sometimes denoted as R_w^2).

to the linearity of the Shultz−Flory distribution, *K* value, and the purity of α-olefins. A conformer with two *ortho*-methyl groups simultaneously above and below the N−Fe(N)−N plane seems to be essential for α-olefin formation with good linearity and purity. It appears that it is not crucial whether the two *ortho*-methyls are from two sides of the aryl imino arms (as in precatalyst **22** of pattern **B**) or come from one side (as in precatalyst **34** of pattern **D**).

In conclusion several precatalysts were synthesized and tested for the oligomerization of ethylene to make linear α-olefins. The goal was to replace complex **1** with a candidate that had a longer lifetime and a more ideal Shultz−Flory product distribu-

Scheme 9. Conformers of Complexes 1, 30, and 22 Resulting upon Rotation of the Aryl Moiety around the Nitrogen−Iron−Nitrogen Coordination Plane

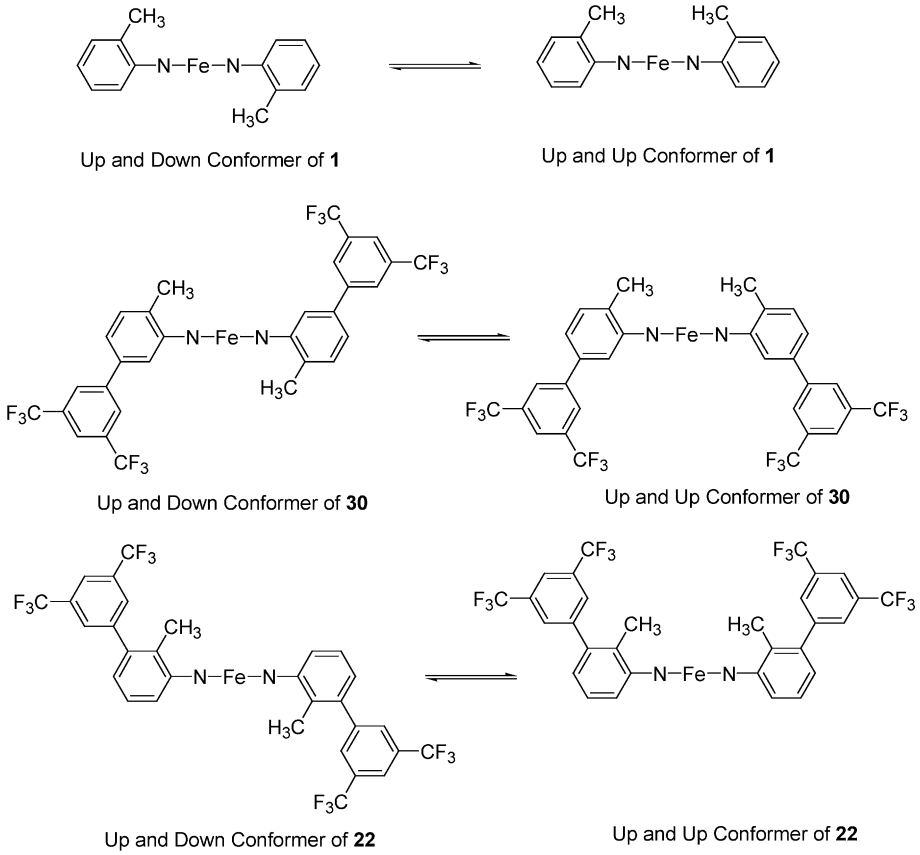

tion. A longer lifetime was observed for nearly all candidates tested. It was also found that the double substitutions of large aryl groups at the *meta* positions in addition to methyls at the *ortho* positions of the imino aryl groups resulted in higher *K* factors, more solids, and a real loss in productivity. Precatalyst **34**, of type **D**, with two *meta*-aryls in one imino aryl group and two *ortho*-methyls in the second imino aryl, had the highest *K* factor of all precatalysts and ranked low in percent solids. This would appear to be a result of the proper combination of steric and electronic factors and conformeric behavior in this type of complex. Future theoretical studies may be beneficial in understanding the correlations between steric and electronic effects and conformeric behavior created by additional substitutions in tridentate ligands and the parameters of the oligomerization processes, and these are under way in our laboratory.

Experimental Section

All air-sensitive compounds were prepared and handled under a N_2/Ar atmosphere using standard Schlenk and inert-atmosphere box techniques. Anhydrous solvents were used in the reactions. Solvents were distilled from drying agents or passed through columns under an argon or nitrogen atmosphere. Anhydrous iron(II) chloride, 1-(6-acetylpyridin-2-yl)ethanone, 3-bromo-2-methylphenylamine, 3,5-dibromo-4-methylphenylamine, 5-bromo-2-methylphenylamine, 4-fluorophenylboronic acid, 3,5-bis(trifluoromethyl)phenylboronic acid, 5-methyl-2-thiopheneboronic acid, tris(dibenzylideneacetone)dipalladium(0), cesium carbonate, di-*tert*-butylchlorophosphine, 2.0 M solution of benzylmagnesium chloride in THF, MMAO, and *n*-butanol were purchased from Aldrich. Complex **1** was prepared according to the literature.[21]

2,6-Bis(1-(3,5-dibromo-4-methylphenylimino)ethyl)pyridine (4). 1-(6-Acetylpyridin-2-yl)ethanone (**2**) (4.39 g, 0.027 mol), 15.0 g (0.057 mol) of 3,5-dibromo-4-methylphenylamine (**3**), 200 mL of the methanol, and a few crystals of *para*-toluenesulfonic acid were stirred for 3 days at room temperature under the flow of nitrogen. The resultant precipitate was filtered, washed twice with 10 mL of methanol, and dried in a 1 mm vacuum overnight. The yield of 2,6-bis(1-(3,5-dibromo-4-methyl)phenylimino)ethyl)pyridine (**4**) was 12.1 g (68%) as a pale yellow solid. ^{1}H NMR (500 MHz, CD_2Cl_2, TMS): δ 2.40 (s, 6H, Me), 2.58 (s, 6H, Me), 7.10 (s, 4H, Arom-H), 7.63 (t, $^3J_{HH}$ = 7.8 Hz, 1H, Py-H), 8.30 (d, $^3J_{HH}$ = 7.8 Hz, 2H, Py-H). ^{13}C NMR (500 MHz, CD_2Cl_2, (selected signals)): δ 169.03 (C=N). Anal. Calcd for $C_{23}H_{19}Br_4N_3$ (MW 657.03): C, 42.04; H, 2.91; N, 6.40. Found: C, 42.21; H, 3.14; N, 6.48.

Di-*tert*-butyl(2,2-dimethylpropyl)phosphane (7). Di-*tert*-butylchlorophosphine (**10**) (28.80 g, 0.160 mol), 0.2 mol of neopentylmagnesium chloride (**11**) in diethyl ether, and 150 mL of THF were refluxed under argon for 3 days. The reaction mixture was allowed to cool to RT, and an aqueous solution of ammonium chloride was added slowly. The organic phase was separated and dried with magnesium sulfate. After removal of the solvent, the product was purified by distillation in a vacuum. The yield of di-*tert*-butyl(2,2-dimethylpropyl)phosphane was 25.26 g (73%) with bp 43−47 °C/0.1 mm. ^{31}P NMR (CD_2Cl_2): +19.76 ppm. ^{1}H NMR (CD_2Cl_2): 1.17 (s, 9H, Me_3C), 1.19 (s, 9H, Me_3C), 2.47 (d, $^2J_{PH}$ = 3.12 Hz, P−CH_2−CMe_3). Anal. Calcd for $C_{13}H_{29}P$ (MW 216.34): C, 72.17; H, 13.51; P, 14.32. Found: C, 72.01; H, 13.49; P, 14.08.

(21) (a) Schmidt, R.; Welch, M. B.; Knudsen, R. D.; Gottfried, S.; Alt, H. G. *J. Mol. Catal A: Chem.* **2004**, *222*, 9. (b) Spence, Rupert; Stevens, Robert Louis. PCT Int. Appl. WO 2005030814, 2005; 20 pp.

2,6-Bis(1-(3,5-di(4-fluorophenyl)-4-methyl)phenylimino)ethyl)pyridine (9). 4-Fluorophenylboronic acid (**5**) (5.62 g, 0.04 mol), 4.4 g (0.0067 mol) of 2,6-bis(1-(3,5-dibromo-4-methyl)phenylimino)ethyl)pyridine (**4**), 13.1 g (0.04 mol) of cesium carbonate (**8**), 0.92 g (0.001 mol) of tris(dibenzylideneacetone)dipalladium(0) (**6**), 0.52 g (0.0024 mol) of di-*tert*-butyl(2,2-dimethylpropyl)phosphane (**7**), and 50 mL of dioxane were stirred at room temperature for 24 h. The reaction mixture was filtered, and the solvent was removed under vacuum. The resulting mixture was purified by recrystallization from 20 mL of methanol. Yield of 2,6-bis(1-(3,5-di(4-fluorophenyl)-4-methyl)phenylimino)ethyl)pyridine (**9**) was 1.53 g (32%) as a light yellow solid. ^{1}H NMR (500 MHz, CD_2Cl_2, TMS): δ 2.10 (s, 6H, Me), 2.45 (s, 6H, Me), 6.60 (s, 4H, Arom-H), 7.12 (m, 4H, Arom-H), 7.35 (m, 4H, Arom-H), 7.80 (t, $^3J_{HH}$ = 7.8 Hz, 1H, Py-H), 8.30 (d, $^3J_{HH}$ = 7.8 Hz, 2H, Py-H). ^{13}C NMR (500 MHz, CD_2Cl_2, (selected signals)): δ 168.0 (C═N). ^{19}F NMR (CD_2Cl_2): −117.00 (s, 4F). Anal. Calcd for $C_{47}H_{35}F_4N_3$ (MW 717.79): C, 78.64; H, 4.91; N, 5.85. Found: C, 78.67; H, 5.19; N, 6.02.

Iron(2$^+$), Bis[2,6-bis(1-(3,5-dibromo-4-methyl)phenylimino)-ethyl)pyridine], Tetrachloferrate(2$^-$) (12). Anhydrous iron(II) chloride (0.17 g, 0.00137 mol) was dissolved in 40 mL of warm *n*-butanol. Then, 1.0 g (0.0015 mol) of 2,6-bis(1-(3,5-dibromo-4-methyl)phenylimino)ethyl)pyridine (**4**) was added in one portion to the reaction mixture. The mixture was kept at 40 °C for 1 h and then cooled to ambient temperature. The resultant purple precipitate was filtered and washed twice with 5 mL of pentane and dried at 1 mm vacuum. The yield of bis[2,6-bis(1-(3,5-dibromo-4-methyl)-phenylimino)ethyl)pyridine]iron(II) chloride (**12**) was 0.74 g (62% of starting ligand). Anal. Calcd for $C_{46}H_{38}Br_8Cl_4Fe_2N_6$ (MW 1567.57): C, 35.25; H, 2.44; N, 5.36. Found: C, 35.30; H, 2.50; N, 5.48. Direct probe MS: calculated top exact mass for $C_{46}H_{38}Br_8Cl_4Fe_2N_6$, 1567.40; found exact mass 1567.40.

Iron(2$^+$), Bis[2,6-bis(1-(3,5-di(4-fluorophenyl)-4-methyl)phenylimino)ethyl)pyridine], Tetrachloferrate(2$^-$) (13). Anhydrous iron(II) chloride (0.17 g, 0.00137 mol) was dissolved in 40 mL of warm *n*-butanol. Then, 1.0 g (0.0014 mol) of 2,6-bis(1-(3,5-di(4-fluorophenyl)-4-methyl)phenylimino)ethyl)pyridine (**9**) was added in one portion to the reaction mixture. The mixture was kept at 40 °C for 1 h and then was cooled to ambient temperature. The resultant purple precipitate was filtered and washed twice with 5 mL of pentane and dried at 1 mm vacuum. The yield of bis[2,6-bis(1-(3,5-di(4-fluorophenyl)-4-methyl)phenylimino)ethyl)pyridine]-iron(II) chloride (**13**) was 0.92 g (78% of starting ligand). Anal. Calcd for $C_{94}H_{70}Cl_4F_8Fe_2N_6$ (MW 1689.09): C, 66.84; H, 4.18; N, 4.98. Found: C, 67.03; H, 4.37; N, 5.24. The structure was proven by X-ray analysis.

2,6-Bis(1-(2-methyl-3-bromophenylimino)ethyl)pyridine (15). 1-(6-Acetylpyridin-2-yl)ethanone (**2**) (18.87 g, 0.116 mol), 45.3 g (0.243 mol) of 3-bromo-2-methylphenylamine (**14**), 300 mL of the toluene, and a few crystals of *para*-toluenesulfonic acid were refluxed with a Dean−Stark trap for 3 days until the calculated amount of the water was separated (4.16 mL) under the flow of nitrogen. The solvent was removed by a rotary evaporator, and the resultant reaction mixture was recrystallized from 50 mL of ethanol. The yield of 2,6-bis(1-(2-methyl-3-bromophenylimino)ethyl)pyridine (**15**) was 47.9 g (83%) as a pale yellow solid. ^{1}H NMR (500 MHz, THF-D_8, TMS): δ 2.15 (s, 6H, Me), 2.33 (s, 6H, Me), 6.67 (m, 2H, Arom-H), 7.35 (m, 4H, Arom-H), 7.90 (t, $^3J_{HH}$ = 7.8 Hz, 1H, Py-H), 8.50 (d, $^3J_{HH}$ = 7.8 Hz, 2H, Py-H). ^{13}C NMR (500 MHz, THF-D_8, (selected signals)): δ 168.0 (C═N). Anal. Calcd for $C_{23}H_{21}Br_2N_3$ (MW 499.24): C, 55.33; H, 4.24; N, 8.42. Found: C, 55.40; H, 4.42; N, 8.46.

2,6-Bis(1-(2-methyl-3-(4-fluorophenyl)phenylimino)ethyl)-pyridine (18). 4-Fluorophenylboronic acid (**5**) (4.71 g, 0.0337 mol), 5.60 g (0.0112 mol) of 2,6-bis(1-(2-methyl-3-bromophenylimino)-ethyl)pyridine (**15**), 10.97 g (0.0337 mol) of cesium carbonate (**8**), 0.77 g (0.00084 mol) of tris(dibenzylideneacetone)dipalladium(0) (**6**), 0.35 g (0.0016 mol) of di-*tert*-butyl(2,2-dimethylpropyl)-phosphane (**7**), and 50 mL of dioxane were stirred at room temperature for 24 h. The reaction mixture was filtered, and the solvent was removed under vacuum. The resulting mixture was purified by recrystallization from 20 mL of ethanol. Yield of 2,6-bis(1-(2-methyl-3-(4-fluorophenyl)phenylimino)ethyl)pyridine (**18**) was 3.74 g (63%) as a light yellow solid. ^{1}H NMR (500 MHz, CD_2Cl_2, TMS): δ 1.95 (s, 6H, Me), 2.40 (s, 6H, Me), 6.63 (m, 2H, Arom-H), 7.40 (m, 14H, Arom-H), 7.91 (t, $^3J_{HH}$ = 7.8 Hz, 1H, Py-H), 8.40 (d, $^3J_{HH}$ = 7.8 Hz, 2H, Py-H). ^{13}C NMR (500 MHz, CD_2Cl_2, (selected signals)): δ 168.1 (C═N). ^{19}F NMR (CD_2Cl_2): −117.32 (s, 2F). Anal. Calcd for $C_{35}H_{29}F_2N_3$ (MW 529.62): C, 79.37; H, 5.52; N, 7.93. Found: C, 79.52; H, 5.69; N, 8.14.

2,6-Bis(1-(2-methyl-3-(3,5-bis(trifluoromethyl)phenyl)phenylimino)ethyl)pyridine (19). 3,5-Bis(trifluoromethyl)phenylboronic acid (**16**) (7.44 g, 0.0289 mol), 4.80 g (0.0096 mol) of 2,6-bis(1-(2-methyl-3-bromophenylimino)ethyl)pyridine (**15**), 9.40 g (0.0289 mol) of cesium carbonate (**8**), 0.66 g (0.00072 mol) of tris-(dibenzylideneacetone)dipalladium(0) (**6**), 0.38 g (0.0018 mol) of di-*tert*-butyl(2,2-dimethylpropyl)phosphane (**7**), and 50 mL of dioxane were stirred at room temperature for 24 h. The reaction mixture was filtered, and the solvent was removed under vacuum. The resulting mixture was purified by recrystallization from 20 mL of ethanol. Yield of 2,6-bis(1-(2-methyl-3-(3,5-bis(trifluoromethyl)-phenyl)phenylimino)ethyl)pyridine (**19**) was 5.14 g (76%) as a light yellow solid. ^{1}H NMR (500 MHz, CD_2Cl_2, TMS): δ 2.05 (s, 6H, Me), 2.41 (s, 6H, Me), 6.68 (m, 2H, Arom-H), 7.05 (m, 2H, Arom-H), 7.30 (m, 2H, Arom-H), 7.95 (m, 7H, Arom-H and Py-H), 8.45 (d, $^3J_{HH}$ = 7.8 Hz, 2H, Py-H). ^{13}C NMR (500 MHz, CD_2Cl_2, (selected signals)): δ 167.7 (C═N). ^{19}F NMR (CD_2Cl_2): −63.54 (s, 12F). Anal. Calcd for $C_{39}H_{27}F_{12}N_3$ (MW 765.63): C, 61.18; H, 3.55; N, 5.49. Found: C, 61.36; H, 3.70; N, 5.52. The structure was proven by X-ray analysis.

2,6-Bis(1-(2-methyl-3-(3-methylthiophene-2-yl)-phenyl)phenylimino)ethylpyridine (20). 5-Methyl-2-thiopheneboronic acid (**17**) (10.0 g, 0.0704 mol), 8.79 g (0.0176 mol) of 2,6-bis(1-(2-methyl-3-bromophenylimino)ethyl)pyridine (**15**), 22.95 g (0.0704 mol) of cesium carbonate (**8**), 1.62 g (0.00177 mol) of tris-(dibenzylideneacetone)dipalladium(0) (**6**), 0.91 g (0.0042 mol) of di-*tert*-butyl(2,2-dimethylpropyl)phosphane (**7**), and 50 mL of dioxane were stirred at room temperature for 24 h. The reaction mixture was filtered, and the solvent was removed under vacuum. The resulting mixture was purified by recrystallization from 20 mL of ethanol. Yield of 2,6-bis(1-(2-methyl-3-(3-methylthiophene-2-yl)phenyl)phenylimino)ethyl)pyridine (**20**) was 3.26 g (35%) as a light yellow solid. ^{1}H NMR (500 MHz, C_6D_6, TMS): δ 2.12 (s, 6H, Me), 2.32 (s, 6H, Me), 2.39 (s, 6H, Me), 6.50 (s, 2H, Arom-H), 6.70 (m, 2H, Arom-H), 7.20 (m, 7H, Arom-H), 8.49 (d, $^3J_{HH}$ = 7.8 Hz, 2H, Py-H). ^{13}C NMR (500 MHz, C_6D_6, (selected signals)): δ 166.6 (C═N). Anal. Calcd for $C_{33}H_{31}N_3S_2$ (MW 533.75): C, 74.26; H, 5.85; N, 7.87. Found: C, 74.29; H, 5.91; N, 7.95.

2,6-Bis(1-(2-methyl-3-(4-fluorophenyl)phenylimino)ethyl)-pyridineiron(II) Chloride (21). Anhydrous iron(II) chloride (0.43 g, 0.0034 mol) was dissolved in 40 mL of warm *n*-butanol. Then, 2.0 g (0.0038 mol) of 2,6-bis(1-(2-methyl-3-(4-fluorophenyl)-phenylimino)ethyl)pyridine (**18**) was added in one portion to the reaction mixture. The mixture was kept at 40 °C additionally for 1 h and then was cooled to ambient temperature. The resultant blue precipitate was filtered, washed twice with 20 mL of pentane, and dried at 1 mm vacuum. Yield of 2,6-bis(1-(2-methyl-3-(4-fluorophenyl)phenylimino)ethyl)pyridineiron(II) chloride (**21**) was 3.83 g (87%). Anal. Calcd for $C_{35}H_{29}Cl_2F_2FeN_3$ (MW 656.37): C, 64.05; H, 4.45; N, 6.40. Found: C, 64.23; H, 4.61; N, 6.48. Direct probe MS: exact mass for $C_{35}H_{29}Cl_2F_2FeN_3$ 655.11; found 655.11.

2,6-Bis(1-(2-methyl-3-(3,5-bis(trifluoromethyl)phenyl)phenylimino)ethyl)pyridineiron(II) Chloride (22). Anhydrous iron-

(II) chloride (0.50 g, 0.0039 mol) was dissolved in 40 mL of warm *n*-butanol. Then, 3.0 g (0.0039 mol) of 2,6-bis(1-(2-methyl-3-(3,5-bis(trifluoromethyl)phenyl)phenylimino)ethyl)pyridine (**19**) were added in one portion to the reaction mixture. The mixture was kept at 40 °C additionally for 1 h and then was cooled to ambient temperature. The resultant blue precipitate was filtered, washed twice with 20 mL of pentane, and dried at 1 mm vacuum. Yield of 2,6-bis(1-(2-methyl-3-(3,5-bis(trifluoromethyl)phenyl)phenylimino)-ethyl)pyridineiron(II) chloride (**22**) was 3.83 g (87%). Anal. Calcd for $C_{39}H_{27}Cl_2F_{12}FeN_3$ (MW 892.38): C, 52.49; H, 3.05; N, 4.71. Found: C, 52.57; H, 3.21; N, 4.96. The structure was proven by X-ray analysis.

2,6-Bis(1-(2-methyl-3-(3-methylthiophene-2-yl)-phenyl)phenylimino)ethyl)pyridineiron(II) Chloride (23). 2,6-Bis(1-(2-methyl-3-(3-methylthiophene-2-yl)phenyl)phenylimino)ethyl)pyridine (**20**) (0.5 g, 0.00094 mol) was dissolved in 30 mL of THF. Then 0.11 g (0.00087 mol) of iron(II) chloride was added in the reaction mixture in one portion. The resultant blue precipitate was filtered after 12 h of stirring, washed twice with 20 mL of pentane, and dried at 1 mm vacuum. Yield of 2,6-bis(1-(2-methyl-3-(3-methylthiophene-2-yl)phenyl)phenylimino)ethyl)pyridineiron(II) chloride (**23**) was 1.34 g (84%). Anal. Calcd for $C_{33}H_{31}Cl_2FeN_3S_2$ (MW 660.50): C, 60.01; H, 4.73; N, 6.36. Found: C, 60.25; H, 4.90; N, 6.39. Direct probe MS: exact mass for $C_{33}H_{31}Cl_2FeN_3S_2$: exact mass 659.07; found exact mass 659.07.

2,6-Bis(1-(2-methyl-3-(3,5-bis(trifluoromethyl)phenyl)phenylimino)ethyl)pyridineiron(III) Chloride (24). 2,6-Bis(1-(2-methyl-3-(3,5-bis(trifluoromethyl)phenyl)phenylimino)ethyl)pyridine (**19**) (1.0 g, 0.0013 mol) was dissolved in 50 mL of THF. Then, 0.20 g (0.0012 mol) of anhydrous iron(III) chloride was added in one portion to the reaction mixture. The mixture was kept stirring for 20 min at ambient temperature. The prolonged stirring caused the reduction of Fe(III) to Fe(II). The resultant orange precipitate was filtered, washed twice with 20 mL of pentane, and dried at 1 mm vacuum. Yield of 2,6-bis(1-(2-methyl-3-(3,5-bis(trifluoromethyl)-phenyl)phenylimino)ethyl)pyridineiron(III) chloride (**24**) was 0.88 g (73%). Anal. Calcd for $C_{39}H_{27}Cl_3F_{12}FeN_3$ (MW 927.84): C, 50.48; H, 2.93; N, 4.53. Found: C, 50.59; H, 3.20; N, 4.57. Direct probe MS: exact mass for $C_{39}H_{27}Cl_3F_{12}FeN_3$ 926.04; found 926.04.

2,6-Bis(1-(2-methyl-5-bromophenylimino)ethyl)pyridine (26). 1-(6-Acetylpyridin-2-yl)ethanone (**2**) (8.33 g, 0.051 mol), 20.0 g (0.107 mol) of 5-bromo-2-methylphenylamine (**25**), and 200 mL of dry toluene with a few crystals of *para*-toluenesulfonic acid were refluxed in a Dean−Stark trap for 3 days until the calculated amount of water was separated (1.84 mL) under a flow of nitrogen. The solvent was removed in a rotary evaporator, and the resultant reaction mixture was recrystallized from 50 mL of ethanol. The yield of 2,6-bis(1-(2-methyl-5-bromophenylimino)ethyl)pyridine (**26**) was 19.88 g (78%) as a pale yellow solid. ^{1}H NMR (500 MHz, C_6D_6, TMS): δ 1.90 (s, 6H, Me), 2.12 (s, 6H, Me), 6.50 (m, 2H, Arom-H), 7.20 (m, 4H, Arom-H), 7.30 (t, $^3J_{HH}$ = 7.8 Hz, 1H, Py-H), 8.40 (d, $^3J_{HH}$ = 7.8 Hz, 2H, Py-H). ^{13}C NMR (500 MHz, C_6D_6, (selected signals)): δ 167.4 (C═N). Anal. Calcd for $C_{23}H_{21}Br_2N_3$ (MW 499.24): C, 55.33; H, 4.24; N, 8.42. Found: C, 55.48; H, 4.45; N, 8.53.

Benzyldi-*tert*-butylphosphane (28). Di-*tert*-butylchlorophosphine (**10**) (75.0 g, 0.415 mol) and 0.5 mol of a 2.0 M solution of benzylmagnesium chloride (**29**) in THF (200 mL) were refluxed under argon for 2 days. The reaction mixture was allowed to cool to RT, and an aqueous solution of ammonium chloride was added slowly. The organic phase was separated and dried with magnesium sulfate. After removal of the solvent, the product was purified by distillation in a vacuum. The yield of benzyldi-*tert*-butylphosphane (**28**) was 94.3 g (96%) with bp 56−59 °C/0.1 mm. ^{31}P NMR ($CDCl_3$): +36.63 ppm. ^{1}H NMR ($CDCl_3$): δ 1.18 (s, 9H, Me_3C), 1.20 (s, 9H, Me_3C), 2.90 (d, $^2J_{PH}$ = 2.92 Hz, P−CH_2−Ph), 7.1−7.6 (m, 5H, aromatic protons). Anal. Calcd for $C_{15}H_{25}P$ (MW 236.33): C, 76.23; H, 10.66; P, 13.11. Found: C, 76.15; H, 10.58; P, 12.87.

2,6-Bis(1-(5-(3,5-bis(trifluoromethyl)phenyl)-6-methylphenylimino)ethyl)pyridine (27). 3,5-Bis(trifluoromethyl)phenylboronic acid (**16**) (10.3 g, 0.04 mol), 5.0 g (0.01 mol) of 2,6-bis(1-(2-methyl-5-bromophenylimino)ethyl)pyridine (**26**), 12.64 g (0.0388 mol) of cesium carbonate (**8**), 0.71 g (0.00078 mol) of tris-(dibenzylideneacetone)dipalladium(0) (**6**), 0.55 g (0.00233 mol) of benzyldi-*tert*-butylphosphane (**28**), and 50 mL of dioxane were stirred at room temperature for 24 h. The reaction mixture was filtered, and the solvent was removed under vacuum. The resulting mixture was purified by recrystallization from 20 mL of ethanol. Yield of 2,6-bis(1-(5-(3,5-bis(trifluoromethyl)phenyl)-6-methylphenylimino)ethyl)pyridine (**27**) was 4.45 g (58%) as a light yellow solid. ^{1}H NMR (500 MHz, C_6D_6, TMS): δ 2.10 (s, 6H, Me), 2.32 (s, 6H, Me), 6.80 (s, 2H, Arom-H), 6.85 (m, 2H, Arom-H), 7.11 (m, 2H, Arom-H), 7.30 (m, 2H, Arom-H), 7.40 (t, $^3J_{HH}$ = 7.8 Hz, 1H, Py-H), 7.60 (s, 2H, Arom-H), 7.80 (s, 4H, Arom-H), 8.50 (d, $^3J_{HH}$ = 7.8 Hz, 2H, Py-H). ^{13}C NMR (500 MHz, C_6D_6, (selected signals)): δ 167.3 (C═N). ^{19}F NMR (C_6D_6): −63.07 (s, 12F). Anal. Calcd for $C_{39}H_{27}F_{12}N_3$ (MW 765.63): C, 61.18; H, 3.55; N, 5.49. Found: C, 61.19; H, 3.50; N, 5.57.

2,6-Bis(1-(5-(3,5-bis(trifluoromethyl)phenyl)-6-methylphenylimino)ethyl)pyridineiron(II) Chloride (30). 2,6-Bis(1-(5-(3,5-bis(trifluoromethyl)phenyl)-6-methylphenylimino)ethyl)pyridine (**27**)-(0.9 g, 0.00118 mol) was dissolved in 30 mL of THF. Iron(II) chloride (0.13 g, 0.001 mol) was added to the reaction mixture in one portion. The resultant blue precipitate was filtered after 12 h of stirring, washed twice with 20 mL of pentane, and dried at 1 mm vacuum. Yield of 2,6-bis(1-(5-(3,5-bis(trifluoromethyl)phenyl)-6-methylphenylimino)ethyl)pyridineiron(II) chloride (**30**) was 0.95 g (83%). Anal. Calcd for $C_{39}H_{27}Cl_2F_{12}FeN_3$ (MW 892.38): C, 52.49; H, 3.05; N, 4.71. Found: C, 52.54; H, 3.14; N, 4.78. The structure was proven by X-ray analysis.

1-{6-[1-(4-Bromo-2,6-dimethylphenylimino)ethyl]pyridin-2-yl}ethanone (31). 1-(6-Acetylpyridin-2-yl)ethanone (22.5 g, 0.138 mol), 25.0 g (0.125) of 4-bromo-2,6-dimethylphenylamine, and 300 mL of *n*-propanol with a few crystals of *p*-toulenesulfonic acid were stirred at room temperature for 36 h in a 500 mL flask under the flow of nitrogen. The resultant yellow precipitate was filtered and washed with 20 mL of methanol. It was then dried at 1 mm vacuum overnight. The yield of 1-{6-[1-(4-bromo-2,6-dimethylphenylimino)ethyl]pyridin-2-yl}ethanone (**31**) was 19.08 g (44%) as a yellow solid. ^{1}H NMR (500 MHz, CD_2Cl_2, TMS): δ 1.95 (s, 6H, Me), 2.22 (s, 3H, Me), 2.30 (s, 3H, Me), 6.80 (s, 2H, Arom-H), 7.95 (t, $^3J_{HH}$ = 8.0 Hz, 1H, Py-H), 8.15 (d, $^3J_{HH}$ = 8.0 Hz, 1H, Py-H), 8.40 (d, $^3J_{HH}$ = 8.0 Hz, 1H, Py-H). ^{13}C NMR (500 MHz, CD_2Cl_2, TMS (selected signals)): δ 168.4 (C═N), 199.5 (C═O). Anal. Calcd for $C_{17}H_{17}BrN_2O$ (MW 345.23): C, 59.14; H, 4.96; N, 8.11. Found: C, 59.18; H, 5.07; N, 8.15.

4-Bromo-2,6-dimethylphenyl-(1-{6-[1-(3,5-dibromo-4-methylphenylimino)ethyl]pyridin-2-yl}ethylidene)amine (32). 1-{6-[1-(4-Bromo-2,6-dimethylphenylimino)ethyl]pyridin-2-yl}ethanone (**31**) (5.0 g, 0.0145 mol), 4.45 g (0.016 mol) of 3,5-dibromo-4-methylphenylamine, 100 g of fresh molecular sieves, and 100 mL of toluene were kept at 90 °C for 3 days under the flow of nitrogen. The solvent was removed by a rotary evaporator, and the residue was recrystallized from 10 mL of ethanol. The yield of 4-bromo-2,6-dimethylphenyl-(1-{6-[1-(3,5-dibromo-4-methylphenylimino)ethyl]pyridin-2-yl}ethylidene)amine (**32**) was 5.75 g (67%) as a yellow solid. ^{1}H NMR (500 MHz, CD_2Cl_2, TMS): δ 1.60 (s, 6H, Me), 2.10 (s, 3H, Me), 2.15 (s, 3H, Me), 2.45 (s, 3H, Me), 6.97 (s, 2H, Arom-H), 7.15 (s, 2H, Arom-H), 7.40 (t, $^3J_{HH}$ = 8.0 Hz, 1H, Py-H), 8.20 (d, $^3J_{HH}$ = 8.0 Hz, 1H, Py-H), 8.40 (d, $^3J_{HH}$ = 8.0 Hz, 1H, Py-H). ^{13}C NMR (500 MHz, CD_2Cl_2, TMS (selected signals)): δ 168.5 (C═N), 164.4 (C═N). Anal. Calcd for

$C_{24}H_{22}Br_3N_3$ (MW 592.16): C, 48.68; H, 3.74; N, 7.10. Found: C, 48.69; H, 3.82; N, 7.17.

4-(3,5-Bis(trifluoromethyl)phenyl)-2,6-dimethylphenyl)-(1-{6-[1-(3,5-(3,5-bis(trifluoromethyl)phenyl)-4-methylphenylimino)-ethyl]pyridin-2-yl}ethylidene)amine (33). 3,5-Bis(trifluoromethyl)-phenylboronic acid (**16**) (9.92 g, 0.0385 mol), 3.80 g (0.0096 mol) of 4-bromo-2,6-dimethylphenyl-(1-{6-[1-(3,5-dibromo-4-methylphenylimino)ethyl]pyridin-2-yl}ethylidene)amine (**32**), 12.54 g (0.0385 mol) of cesium carbonate (**8**), 0.88 g (0.00096 mol) of tris-(dibenzylideneacetone)dipalladium(0) (**6**), 0.50 g (0.0023 mol) of di-*tert*-butyl(2,2-dimethylpropyl)phosphane (**7**), and 50 mL of dioxane were stirred at room temperature for 24 h. The reaction mixture was filtered, and the solvent was removed under vacuum. The resulting mixture was purified by recrystallization from 20 mL of ethanol. Yield of 4-(3,5-bis(trifluoromethyl)phenyl)-2,6-dimethylphenyl)-(1-{6-[1-(3,5-(3,5-bis(trifluoromethyl)phenyl)-4-methylphenylimino)ethyl]pyridin-2-yl}ethylidene)amine (**33**) was 5.14 g (76%) as a light yellow solid. ^{1}H NMR (500 MHz, CD_2Cl_2, TMS): δ 1.55 (s, 3H, Me), 1.90 (s, 6H, Me), 2.30 (s, 3H, Me), 2.49 (s, 3H, Me), 6.40 (s, 2H, Arom-H), 6.97 (s, 2H, Arom-H), 7.15 (s, 2H, Arom-H), 7.40 (t, $^3J_{HH}$ = 8.0 Hz, 1H, Py-H), 7.60 (s, 4H, Arom-H), 8.20 (d, $^3J_{HH}$ = 8.0 Hz, 1H, Py-H), 8.40 (d, $^3J_{HH}$ = 8.0 Hz, 1H, Py-H). ^{13}C NMR (500 MHz, CD_2Cl_2, (selected signals)): δ 168.0 (C═N), 167.2 (C═N). ^{19}F NMR (CD_2Cl_2) δ −62.96 (s, 12F), −63.00 (s, 6F). Anal. Calcd for $C_{48}H_{31}F_{18}N_3$ (MW 991.75): C, 58.13; H, 3.15; N, 4.24. Found: C, 58.25; H, 3.18; N, 4.30.

4-(3,5-Bis(trifluoromethyl)phenyl)-2,6-dimethylphenyl)-(1-{6-[1-(3,5-(3,5-bis(trifluoromethyl)phenyl)-4-methylphenylimino)-ethyl]pyridin-2-yl}ethylidene)amineiron(II) Chloride (34). 4-(3,5-Bis(trifluoromethyl)phenyl)-2,6-dimethylphenyl)-(1-{6-[1-(3,5-(3,5-bis(trifluoromethyl)phenyl)-4-methylphenylimino)ethyl]pyridin-2-yl}ethylidene)amine (**33**) (0.5 g, 0.0005 mol) was dissolved in 20 mL of THF. Then 0.064 g (0.0005 mol) of iron(II) chloride was added to the reaction mixture in one portion. The resultant blue precipitate was filtered after 12 h of stirring, washed twice with 20 mL of pentane, and dried at 1 mm vacuum. Yield of 4-(3,5-bis-(trifluoromethyl)phenyl)-2,6-dimethylphenyl)-(1-{6-[1-(3,5-(3,5-bis-(trifluoromethyl)phenyl)-4-methylphenylimino)ethyl]pyridin-2-yl}-ethylidene)amineiron(II) chloride (**34**) was 0.95 g (83%). Anal. Calcd for $C_{48}H_{31}Cl_2F_{18}FeN_3$ (MW 1118.50): C, 51.54; H, 2.79; N, 3.76. Found: C, 51.57; H, 3.02; N, 3.94. The structure was proven by X-ray analysis.

General Conditions of the Oligomerizations. Ethylene oligomerizations are done in a 1 L stainless steel Autoclave Engineering Zipperclave. Catalyst and cocatalyst are charged separately using stainless steel injection tubes. The complexes **1**, **21**, **22**, **23**, **24**, **30**, and **34** are activated by modified methylaluminoxane (MMAO). The steps for a typical oligomerization follow. The injectors are charged in a glovebox. The cocatalyst is obtained as a 7 wt % solution of aluminum in *o*-xylene and is charged as such into the injector assembly along with a 10 mL chase of *o*-xylene. The catalysts are prepared as suspensions in *o*-xylene (10 mg/100 mL). A sample is pulled from a well-stirred suspension and is added to a 10 mL charge of *o*-xylene. The injectors are attached to autoclave ports equipped with dip tubes. Nitrogen is sparged through the loose fittings at the attachment points prior to making them tight. The desired charge of *o*-xylene is then pressured into the autoclave. The agitator and heater are turned on. When the desired temperature is reached, the cocatalyst is charged to the clave by blowing ethylene down through the cocatalyst injector. After a significant pressure rise is seen in the autoclave to indicate the cocatalyst and chase solvent have entered, the injector is isolated from the process using its valves. The pressure controller is then set to 5 psig below the desired ethylene operating pressure and is put in the automatic mode to allow it to control the operation of the ethylene addition valve. When the pressure is 5 psig below the desired operating pressure, the controller is put into manual mode and the valve is set to 0% output. When the batch temperature is stable at the desired value, the catalyst is injected using enough nitrogen such that the reactor pressure is boosted to the desired pressure. At the same time as the catalyst injection, the pressure controller is put in the automatic mode and the oligomerization is underway. The 5 psi boost is obtained routinely by having a small reservoir between the nitrogen source and the catalyst injector. A valve is closed between the nitrogen source and the reservoir prior to injecting the catalyst, so the same volume of nitrogen is used each time to inject the catalyst suspension. To stop the oligomerization, the pressure controller is put into manual, the ethylene valve is closed, and the reactor is cooled. The reaction time is 1 h.

Acknowledgment. The authors wish to thank Dr. Jerald Feldman for proofreading the manuscript.

Supporting Information Available: Crystallographic information (CIF file) for compounds **1**, **13**, **15**, **22**, **30**, and **34**. These materials are available free of charge via the Internet at http://pubs.acs.org.

OM051069O